VNIVERSITAT DE VALÈNCIA Facultat de Física

Máster en Física Avanzada

Especialidad Física Teórica

Trabajo Fin de Máster

STUDY OF LONG LIVED PARTICLES BEYOND THE STANDARD MODEL AT LHCB

Miguel Jiménez Ortega

Tutora: Arantza Oyanguren

Curso académico 2021/22

Abstract

Long-lived particles are predicted in many extensions of the Standard Model but the experimental detection is very challenging because they decay out of the first trackers and usually scape to the trigger decisions. In this work we review several new physics models and summarize the experimental status concerning the related searches. We revise the capabilities of the high level trigger system of the LHCb experiment and evaluate the effect of the trigger to detect long-lived particles for two models: a previous work where Dark Higgs Model is assumed, and another one studied for first time in this work, the Composite Higgs involving light scalars signatures. A Montecarlo study about the decay vertex proportions at reconstructible level is conducted, giving a general idea of how much information is missing from tracks downstream of the LHCb magnet. In the case of Composite Higgs model, a 60% of this type of vertices can be missed for lifetimes larger than 10 ps.

Contents

Acknowledgments

Firstly I would really like to thanks my supervisor Arantza Oyanguren, for her implication in this work and for giving me advise when a I needed. Also to all those people enrolled inside IFIC-LHCb group. On the other hand, I have to thanks Elena Dall'Occo, Xabier Cid Vidal, Pieter David, Emma Torró, Joannis Papavassiliou, Emilio Xose Rodriguez Fernandez, Claudia Hagedorn, Santiago de la Hoz and Pepe Navarro for helping me out in both theoretical and experimental stuff for the achievement of this project, I really appreciate it. Thank you so much to my Master mates, also to all those professors which help me in whatever I demanded. And last but not least, thanks my friends Diego, Pedro, Manu y Arturo for supporting me and also to my parents, my biggest support.

1 Introduction.

The particle physics world has been working to find physics beyond The Standard Model (SM) in last decades. The SM shows itself as very good phenomenological theory well understood at scales below TeV. But as other physics theory, it contains some aspects which has not been able to explain properly or some problems which lightly destabilize the theoretical framework: naturalness, the origin of neutrino's masses, matter-antimatter universe asymmetry, dark matter, gravity, etc. This is why some theoretical extensions have been made for years in order to solve this and also to provide new signatures to look for in the next generation of detectors. One of the most encouraging signatures are the so-called Long-Lived particles (LLPs) which arise as particles with Long lifetime which don't leave hits in all subdetectors of a specific particle physics detector. In figure 1 we have an schematic picture of the SM particles classified attending to the fact that if they decay promptly or not. Sometimes these

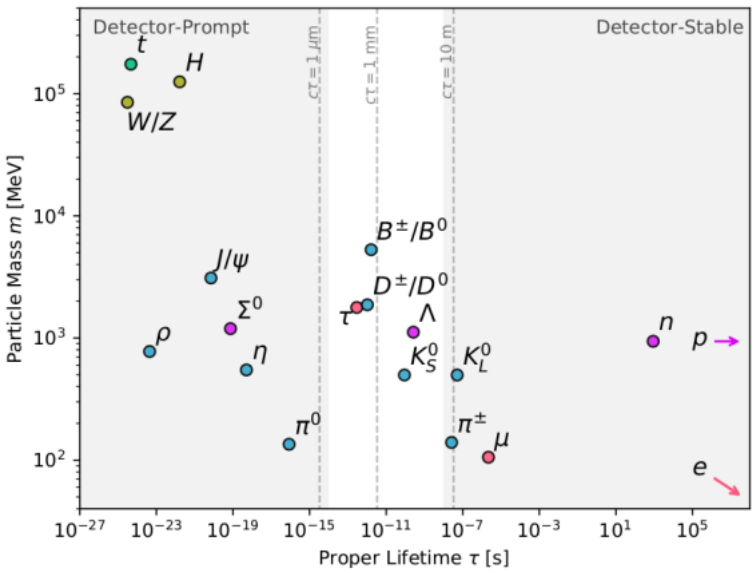

Figure 1: SM particle spectrum as a function of mass and proper lifetimes.

particles can have a lifetime larger than the spatial acceptance of the detector.The aim in the next generation of detectors is trying to detect such exotic particles in order to prove different models of physics Beyond Standard Model (BSM) currently proposed. This work is highly focused on the LHCb experiment. In Section 2 we give a brief review of the main features of the technical part and trigger of LHCb detector for the next data taming period. In Section 3 we explore some of the most encouraging theoretical models which support the actual LLPs searches, mainly focused on the

LHCb case. In Section 4 we review the actual and the most well-motivated searches of LLPs inside the LHCb experiment. In Section 5.2 we perform a complete study of an specific channel $B^+ \to K^+ a_1 a_2$, beyond the SM, looking for long-lived particles as the light scalars a_1 and a_2. Finally we give a general summary of the main conclusions of this work in Section 6.

2 The LHCb detector.

The LHCb detector is one of the detectors of the Large proton-proton Collider (LHC) located at CERN. In this work we focus on the search of long lived particles (LLP) in this detector. We discuss now the main technical and online features of such detector. Since in the incoming Run III of LHCb the LHC will be able to reach $\sqrt{s} = 14$ TeV energies and work with an instantaneous luminosity $2 \times 10^{33} \text{cm}^{-2}\text{s}^{-1}$, a new upgrade of the LHCb system has been achieved. The two main changes can be summarized as follows: the upgrade of the technical setup and the one for the online systems, specially focused on the trigger system.

2.1 Detector technical setup.

The LHCb detector is a single-arm spectometer oriented in the forward direction which is focused on studying heavy flavour physics. Its angular coverage runs from 15 mrad to 300 (250) mrad in the horizontal (vertical) plane. An sketch of the general setup is shown in figure 2 [1]. The main purpose of this detector is searching for evidences of new physics in measurements of CP violation or rare decays of beauty and charm hadrons for different channels. Since the $b\bar{b}$ and $c\bar{c}$ mesons at high energy are very boosted in the longitudinal direction, the geometry of this detector allows us to collect a large amount of pairs inside geometrical acceptance. The upgraded detector can be divided in different subdetectors which play a fundamental role in order to measure different signatures. The parts of the detector can be classified as:

- A spectrometer magnet which is capable of deflecting charged particles in the transversal plane. The field generated reachs up to 4 Tm. The momentum of such particles can be measured making use of it. The arised Lorentz's force bends the particle trajectories. This allows us to determine the momentum of such particles.

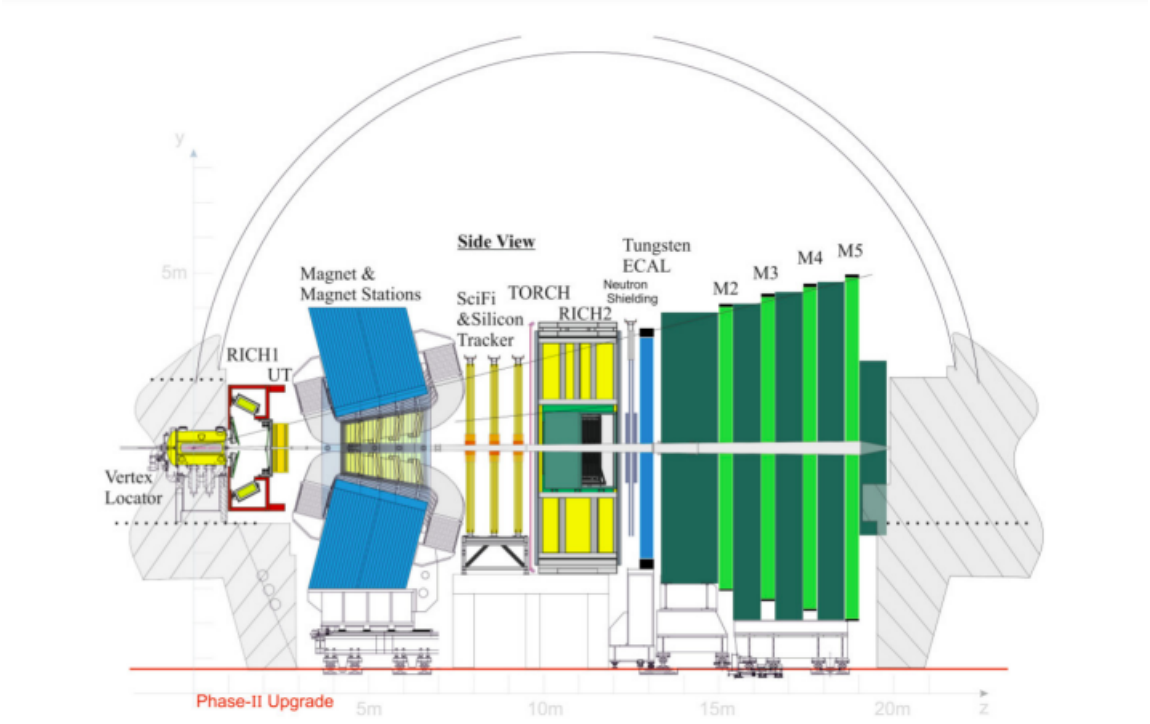

Figure 2: Schematic side-view of the upgrade I detector.

- We also have a tracking system which reconstruct trajectories of charged particles by matching hits in different subdetectors. A hit efficiency of 99% is usually reached. Different trackers appears in the upgraded detector [2]:
  - The Vertex Locator (VELO) consists in pixel technology detector type, such tracker stays near interaction region. High spatial resolution is provided both for the measurement of the radial and the azimutal coordinates. In this way, precise flight directions and vertex positions can be done accurately.
  - The Upstream Tracker (UT) is a silicon strip detector located before the magnet dipole. The previous detector Tracker Turicensis (TT) was replaced by this one for the upgrade I. The role of this detector is crucial in order to measure the particles' momentum together with VELO.
  - The Scintillating Fibre Tracker (SciFi) is located after the magnet dipole. SciFi is composed of 2.5 m long fibres read out by silicon photo-multipliers (SiPMs) outside the acceptance. Its 12 scintillating fibres detection planes are arranged in 3 stations. This detector is the substitute of the original three downstream tracking (T-)stations. The purpose of this detector is to provide hit positions of particles in order to perform the pattern recognition with high efficiency.

- RICH-type detectors (RICH1 and RICH2) are also included in this setup. These ones will provide measurements of charged hadrons. The range covered runs from 2 to 100 GeV/c.

- Electromagnetic calorimeter (ECAL) and hadronic calorimeter (HCAL) plays the role of measuring the deposited energy of both charged and neutral particles.

- The muon detection system (M2-M5) is focused in detecting muon's tracks. A minimum value for momentum (6 GeV/c) is demanded in order to cross all stations.

2.2 Detector trigger.

One of the limitations of this detector before the upgrading program was that the collision rate had to be reduced to the readout rate of 1.1 MHz within a fixed latency. In order to solve this problem, an upgrade of the trigger system has been carried out. A brief general scheme of the trigger is shown in figure 3 [3]. Here we have the different steps taken by the trigger in order to make a correct selection of events. One of the most important things that the trigger takes into account in order to make selections is the particle's track-type among other variables. The different tracks which we can reconstruct in this detector are schematically shown in figure 4 [4]. We can classify them as follows:

- Long tracks. These tracks are associated to particles generated inside VELO which can go through the full detector. Even though they can give hits in all the subdetectors, usually the hits in VELO and SciFi detectors are used to match the tracks.

- Upstream Tracks. These particles come from VELO and are deflected by the magnet. They are useful to reconstruct low momentum particles which don't reach to SciFi.

- Downstream Tracks. These tracks are supposed to be created around UT, after the VELO, so they don't leave hits on the tracker. They are also deflected by the magnet and can leave hits in SciFi.

- VELO Tracks. This type of tracks are created inside VELO and they do not reach the other sub-detectors.

- T Tracks. These ones are those tracks which only hit SciFi. The reconstruction of such tracks take a large time for the identification algorithm.

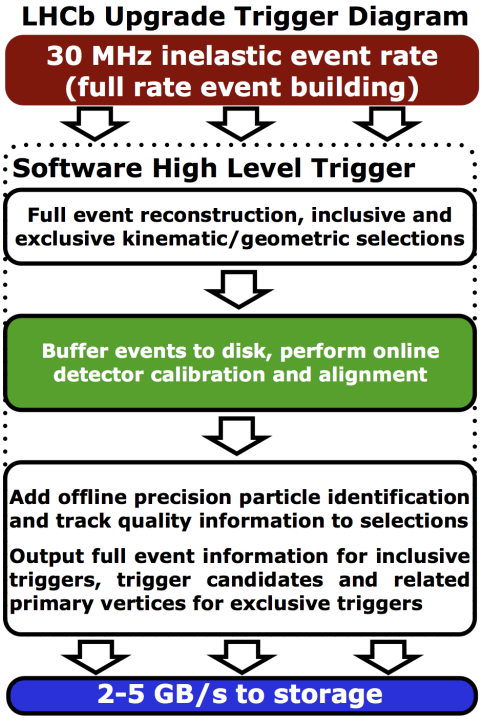

Figure 3: General scheme of how the trigger after upgrade I works.

The basic scheme of the trigger event selection is based on the quick identification of interesting and useful track events. After upgrade I, in Run III, the LHC is supposed to work with an instantaneous luminosity of $2 \times 10^{33} \text{cm}^{-2}\text{s}^{-1}$ and CM frame energy for pp collisions of $\sqrt{s} = 14$ TeV. The trigger system will receive bits from detector at 30 MHz. From this amount of data, the trigger will have to be capable of selecting useful events. This goal is achieved by means of the upgrade I described in the Technical Design Report (TDR) for online setup [5]. The architecture of such trigger is based on two parts: the Low Level Trigger (LLT) and the Higher Level Trigger (HLT). The LLT is essentially the Run 1 Level-0 hardware trigger modified to run within the new readout system. Its work consists in identifying events containing clusters with high transverse energy in the calorimeters or tracks with high transverse momentum in the muon detector [5]. The HLT part, which is actually the one represented in figure 3, consists of two steps: HLT1 and HLT2. HLT1 takes decisions in order to reduce the 30 MHz collision rate to 1 MHz. It takes into account variables as: Primary vertices, long tracks, muon tags, PID (Particle Identification),... in order to perform the event reconstructions. This data is also used to perform a real-time calibration and

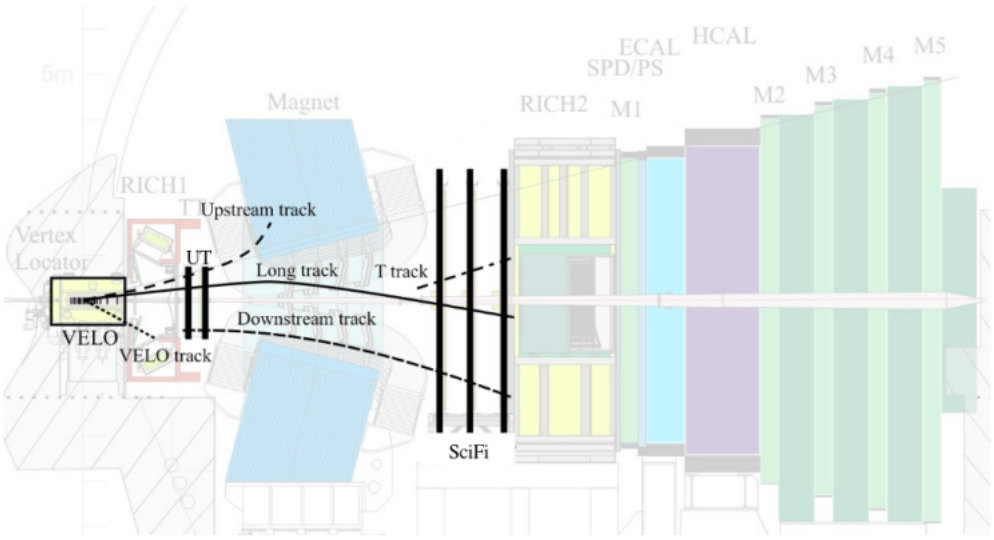

Figure 4: Track types in the LHCb detector. The different subdetectors after upgrade I are also shown.

alignment of the detectors. There are two main parts which holds the HLT1 efficiency: Trigger Independent of the Signal (TIS) and Trigger on signal (TOS). In TIS the trigger decision is not based on variables of the signal considered. On the other hand, in TOS the trigger decision relies on the decay products of the specific signal studied. The next stage in the trigger process is HLT2. It works with 1 MHz event rate coming from HLT1 selections. More variables are involved in such selection, only Downstram tracks together with Long tracks are used in the selection. Nevertheless, not only Downstream tracks are reconstructed, but also T-Tracks. At this point the data can be saved as 'Turbo' or 'Fullstream'. Those data saved as 'Turbo' is only keeping few light objects (tracks) meanwhile 'Fullstream' is saving everything (all the bits), so events are very heavy.

For further knowledge, we will present in this work some analysis related to different vertex proportions. In this way, we need to know what kind of displaced vertices we expect to find when the reconstruction is made. There are three types of vertices: LL, DD and TT. They depend on the position where the searched particle decays. An illustrative representation is shown in figure 5. As we see, all those which decay in VELO are LL, the ones which decay between the final of VELO and UT are DD and the ones between UT and Scifi are called TT.

On the other hand, as we are going to show some HLT1 efficiency plots, some information about the efficiency of this trigger step is needed. For any specific channel

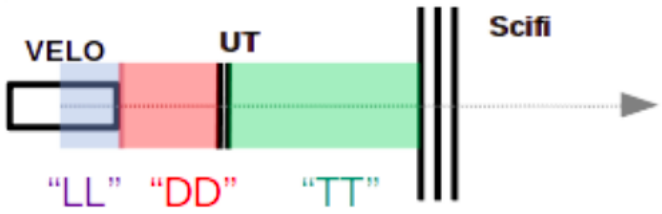

Figure 5: Classification of different displaced vertices depending on Z coordinate at true level.

like $B \to Ka_1$, where a_1 is a lorentz scalar which will be the cornerstone of our study in the Composite Higgs Model, we will have two main contributions to the HLT1 efficiency. This two contributions are the Trigger On the Signal (TOS) and the Trigger Independent of the Signal (TIS). In the first one the decision of reconstructibility of the event does depend on the decay products of the specific channel where B is involved. We can trigger both on the Kaon and on the Scalar a_1, and this will give us different efficiencies for HLT1. For the other one, the decision relies on all those variables of the signal which is not considered. In our study, we will investigate triggering on a_1 to get a true idea of the HLT1 efficiency in this model.

3 Models BSM concerning LLPs.

Several models show up when we talk about Physics Beyond Standard Model (BSM). In this work we mainly follow the MATHUSLA's paper [6] where several theoretical models are studied. We focus on models such as SUSY (specially Dark Photon and Super Gravity models with R-parity violation) and Hidden Valleys. Also, even though we write down here about some models, we also focus on specific searches like resonances $\mu^+\mu^-$ [7] or LLP decaying to $e^\pm\mu^\pm\nu$ [8] where different types of frameworks are involved.

3.1 Dark Photon model.

Among the different solutions which BSM models are capable of providing, maybe the minimal Dark Photon model is the easiest and most extended. In this simple model an extra symmetry group $U(1)_D$ which interacts with SM is considered. The

basic idea consists of providing a natural 'portal' coupling between the Dark sector and the SM [9]. In this section we detail two possible searches for Dark Photons taking into account that the production can come either from virtual particles, so in this way we get portals between Dark sectors and SM, or from direct couplings between both sectors. If the coupling of such vertices are small enough we can get the Dark Photon to be long-lived.

3.1.1 Searches for visible Dark Photon.

In this model we consider an extra symmetry group $U(1)_D$ which directly interacts with the SM. In order to produce this dark boson, several scenarios can be researched. The simplest one is where a 'kinetic mixing' with the SM photon appears, in such a way:

$$\mathcal{L} = \frac{1}{2}\epsilon F^{\mu\nu} F'_{\mu\nu}. \tag{3.1}$$

Here the F and F' terms are related to the field strength tensors associated to $U(1)_Q$ and $U(1)_D$ respectively, where Q is the usual electromagnetic charge. The dimensionless parameter ϵ is supposed to take a value around $10^{-4} \sim 10^{-2}$ in theories where the leading contribution is at one loop, or $10^{-6} \sim 10^{-3}$ for Grand Unification Theories (for instance) where such one-loop contribution vanishes and we need to reach up to order two. These kind of searches are called 'visible' because the Dark Photon interact with SM giving rise to A' decays to SM particles [1]. Namely, it is assumed that A' is the lightest dark particle, so it has necessarily to decay into SM particles. Some of the channels where the Dark Photon is involved might be interesting in the case of the LHCb. In figure 6 we can see the different BR for all these channels. In the low mass regime two important channels dominate, the ones in which we have $\mu^+\mu^-$ and e^+e^- which is a recent improved channel in the case of the LHCb [11]. Of course these channels hold if decays of the Dark Photon to possible dark-sector states are kinematically forbidden. In order to give a concrete example, in the case where $m_{A'} > 2m_l$, where l is the lepton, if we consider A' as the dark boson, the decay width into SM leptons for such boson reads:

$$\Gamma(A' \longrightarrow ll) = \frac{1}{3}\epsilon^2\alpha \left(1 + \frac{2m_l^2}{m_{A'}^2}\right)\sqrt{m_{A'}^2 - 4m_l^2} \tag{3.2}$$

For small ϵ coupling values, such Dark Photon can be long-lived, this is shown

[1] In the canonical form, the lagrangian term reads $\mathcal{L} = \epsilon e A'_\mu J^\mu_{EM}$ which gives rise to a highly predictive theory. See for instance some examples from reference [10]

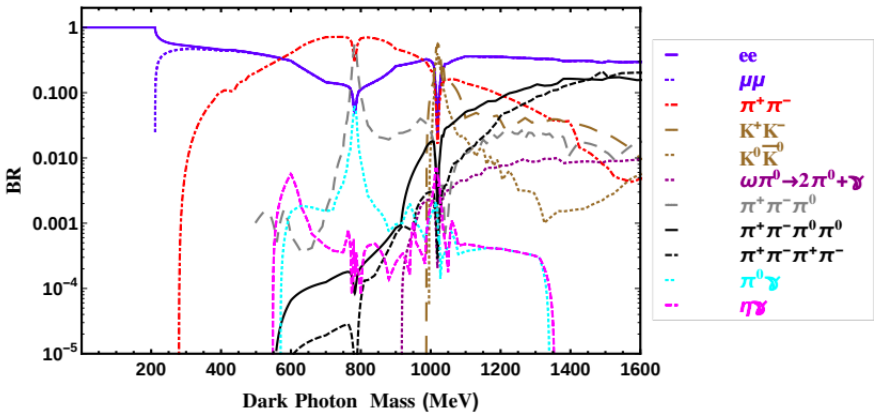

Figure 6: Visible Dark Photon Branching ratios for different channels. Taken from [9].

in figure 7 reported by MATHUSLA collaboration. Even for $m_{A'}$ large masses the traveled distance of the A' before decaying can be several meters.

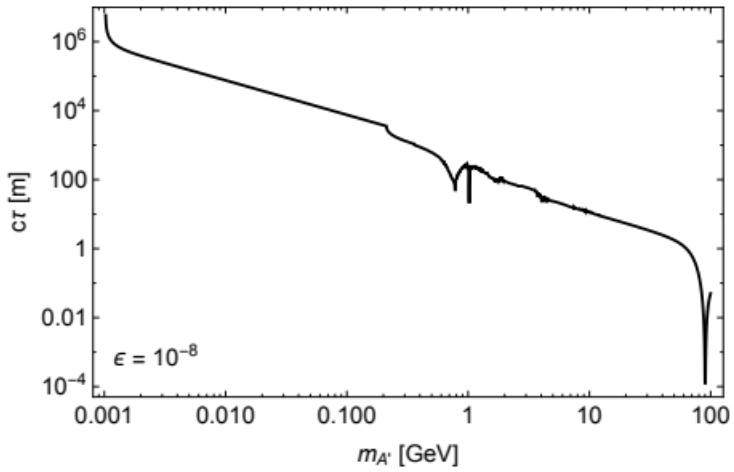

Figure 7: Dark Photon lifetime for $\epsilon = 10^{-8}$ when A' can only decay to SM particles. $c\tau$ scales as ϵ^{-2} . Taken from [6].

3.1.2 Searches for invisible Dark Photon.

Some extensions of the SM where Dark sectors are involved defend that the interaction between Dark sector and the SM is hidden. This means that there is some 'virtual' particle which couples both to SM and Dark sector. This particle is usually called 'mediator'. From theoretical arguments, one expects the most relevant interac-

tions to come from 'renormalizable portals' where SM gauge singlet operators with mass dimension less than or equal to 4 arise. Inside different options of such interactions, the coupling making use of the hypercharge strength field ($B_{\mu\nu}$) seems to be the most well-motivated for DM searches, specially for light dark matter scenarios. This leads to a theoretical framework where the mediator is a vector field. Analogously to previous section, here the Lorentz invariant kinetic mixing interaction reads:

$$\mathcal{L} \sim \epsilon_Y B^{\mu\nu} F'_{\mu\nu}, \tag{3.3}$$

which is gauge invariant. In the end, in this framework we consider A' to not be the lightest dark particle. The Spontaneous Symmetry Breaking at Electroweak Scale gives rise to the term $\epsilon F^{\mu\nu} F'_{\mu\nu}$, coming from eq. (3.3), which indeed looks like eq. (3.1). If the Dark Photon is massive the $U(1)_D$ symmetry must be broken. The most intuitive approach can be the Hidden Abelian Higgs Model [12]. In this way, a dark higgs h_D comes out. It is expected to be mixed with the SM higgs in such a way:

$$\mathcal{L} = \kappa |h_D|^2 |H|^2, \tag{3.4}$$

which at the end give us a new channel where the Dark Photon can be produced coming from rare Higgs decays.

3.1.3 Signatures of dark photons.

Several channels may be pointed out in order to look for A' signatures both for visible or invisible scenarios. Some of the most well-motivated productions are bremsstrahlung of the Dark Photon during gluon-gluon collision, exotic Higgs decay to two Dark Photons via mixing with the dark Higgs or meson decays. The Feynman diagrams for such processes are shown in figure 8. In the case where only kinetic mixing is considered, the dominant production mechanism for Dark Photons, as long as the Dark Photon mass is below the meson mass, is the meson decays. The most important meson decays are pion and eta decays. In this case, the total decay width can be also estimated as MATHUSLA collaboration does, which looks like:

$$\Gamma \sim \frac{\alpha_D \alpha \epsilon^2}{18\pi} \frac{m_D^5}{m_{A'}^4}, \tag{3.5}$$

which might give rise to long life-times depending of the values of the parameter space. At the end of the day we see in these models a potential framework where several signals for new physics can be reached. Some extensions of this model can be found in the literature, like Dark Photons decaying to LLP's and beyond.

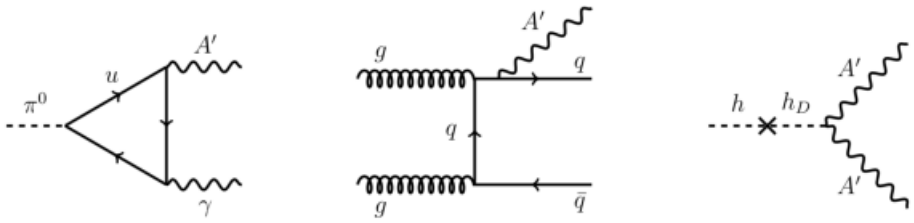

Figure 8: Examples of the Feynman diagrams for Dark Photon production at the LHC. Left: pion decay to the dark photon and a SM photon. Middle: bremsstrahlung of the Dark Photon during gluon-gluon collision. Right: exotic Higgs decay to two Dark Photons via mixing with the dark Higgs.

3.2 Composite Higgs Model.

3.2.1 The problem of Naturalness.

Composite Higgs model is one of the models which solve the problem of naturalness[2] inside the Standard Model (SM). Such problem comes from the fact that the Higgs mass is not protected by any symmetry and it is very sensitive to quadratic quantum corrections. Following the 'Naturalness criterion' the Higgs boson seems to be 'unnatural' inside SM. If we want to compute the value of the physics mass of the Higgs, we should perform the integral:

$$m_H^2 = \int_0^\infty dE \frac{dm_H^2}{dE}(E; p_{true}), \tag{3.6}$$

where p_{true} makes reference to the input parameters for a 'complete' and 'true' theory, beyond the SM[3]. This expression stands for the contribution of virtual quanta with a given energy E. If we separate such integral by means of the cutoff Λ_{SM} in which the SM is supposed to be 'valid' as an effective theory, the two contributions read:

$$m_H^2 = \int_0^{\lesssim\Lambda_{SM}} dE \frac{dm_H^2}{dE}(E; p_{true}) + \int_{\lesssim\Lambda_{SM}}^\infty dE \frac{dm_H^2}{dE}(E; p_{true}). \tag{3.7}$$

Since these two contributions come from different energy scales, they are supposed to be unrelated. On the other hand, the experimental mass of the Higgs has a fixed value (~ 125 GeV/c^2). Such light mass value demands the condition $\delta_{SM} m_H^2 \approx -\delta_{BSM} m_H^2$[4]

[2]For an extended discussion about this topic, I highly recommend the reference [13].

[3]We mean with the expressions 'true' and 'complete' theory to the one which could be capable of predicting the real physics beyond the SM.

[4]Note here we rewrote the two contributions of the integral in a compact form. The first one comes from the SM and the second one from some 'true' theory beyond SM.

to be fulfilled. In order to achieve this, we need a very accurate cancellation. If we define the tunning as $\Delta = \frac{\delta_{SM} m_H^2}{m_H^2}$, we find that for a typical scale value of $\Lambda_{SM} \approx M_{GUT}$ the tunning value is around $\Delta \gtrsim 10^{24}$. This means that in the 'true' theory formula for m_H, a 24 digits cancellation is taking place among two 'a priori' unrelated terms [14]. This statement is at least suspicious, apart from the fact that this type of accuracy will be rather difficult to achieve. The predictive power of new theories taking into account this problem will be poor. Several solutions can be proposed to solve this, we focus on the solution provided by Composite Higgs Model in this section [13].

3.2.2 The basic assumptions of Composite Higgs Model.

In order to have a 'realistic' theory we need at least two ingredients: we need to solve the problem of the naturalness in a proper way and we need to get back in some limit the usual SM theory. For the first one, the solution proposed by the Composite Higgs Model is to assume that the Higgs boson is no longer a point-like particle, but rather a 'composite' system with an specific geometrical size l_H. The Higgs boson is then assumed to be a bound state of a new strong force characterized by a confinement scale $m_* = 1/l_H$. In this way, the problem of naturalness can be solved. Since the low energy quanta have very high wavelength, they are not capable of resolving the size of the Higgs boson. So in this case the dependence between the energy and the integrand is linear, such as in the SM. This linear behaviour gives rise to quadratically dependences with the upper limit cutoff. But as we get closer to the scale m_*, these divergences are canceled out by the finite size effects of the Higgs boson. At this point the linear dependence is turned into a peak around $E \sim m_*$, and after it, the behaviour is a quick fall. Therefore the Higgs mass is no longer sensitive to high energy quadratic corrections and the problem of naturalness is solved [5]. For the second ingredient, the main idea is to assume two sectors, named: 'Composite Sector' and 'Elementary Sector'. The composite sector respects a general global symmetry $\mathcal{G}$ which is spontaneously broken at a scale of $f \sim$TeV. This global symmetry contains $SU(2)_L \times U(1)_Y$ as a subgroup. The W_μ and B_μ fields can make the $SU(2)_L \times U(1)_Y$ group local making use of the usual gauge procedure. Namely, we couple them to the conserved current of the composite sector by means of $\mathcal{L}_{int}$, in strongly analogy to the QCD construction where the general symmetry would be the chiral symmetry[6]

[5] As it is mentioned in reference [14], we need to be sure that this mechanism does not provide a new naturalness problem at TeV scale, something that can be solved following the discussion therein.

[6] Notice that this is just an analogy, it is not exactly the same since the chiral symmetry is explicitly broken by the quark masses in the QCD construction.

[14]. That is how we get a communication channel between the elementary and the composite sectors. A general picture of this theory construction is shown in figure 9. As we can see, the elementary sector is indeed the usual SM framework but without the Higgs and the right-handed top quark t_R. The no inclusion of t_R in this set will be explained later on, with the assumption of the 'Partial Compositeness' hypothesis. The usual procedure to generate the Higgs is the following. The general symmetry group $\mathcal{G}$ is spontaneously broken by the 'Elementary Sector' $\mathcal{H}$ at certain scale f giving rise to Nabu-Goldstone Bosons (NGBs) in the $\mathcal{G}/\mathcal{H}$ coset. The Higgs here is presented as a pseudo NGB since the Goldstone's Theorem is not completely fulfilled because $\mathcal{G}$ is explicitly broken and the NGBs can be massive. After the first breaking, with the Higgs being the usual one in the SM, the Electroweak spontaneous symmetry breaking (EWSSB) takes place. So two symmetry breaks are provided by this theory, the relation between both 'breaking' scales is what usually called as 'Vacuum misalignment' $\xi = sin^2\theta = \frac{v^2}{f^2}$ where v is the usual EWSSB scale $v \sim 246$ GeV. Note that in the limit $\xi \to 0$ we recover the SM, as this limit the composite sector decouples and the Higgs boson turns effectively into an elementary particle. The next step in this framework is to know how to introduce the matter of the fermions. In this case, two ways arise, the ancient technicolor theories [15] and the 'Partial Compositeness' hypothesis intially proposed by D. B. Kaplan [16]. 'Partial Compositeness' hypothesis is based on the idea that SM states come from the mixing between composite and elementary sector degrees of freedom in such a way:

$$|SM\rangle_i = sin\theta\,|Composite\rangle_i + cos\theta\,|Elementaty\rangle_i\,, \tag{3.8}$$

the yukawa couplings coming from this framework read [14] :

$$y_f = g_* sin\theta_R^f sin\theta_L^f, \tag{3.9}$$

where g_* is the typical coupling constant for the composite sector. As we see, since the top has a large yukawa coupling, it is necessarily composite, namely, $sin\theta \sim 1$, unlike the rest of light leptons, which are partial composite. As a final comment, we must be aware of the fact that $\mathcal{L}_{int}$ must remain a weak perturbation of the composite sector dynamics in order to break $\mathcal{G}$ but also not to change the hierarchy between m_* and Λ_{UV}[7].

[7] Λ_{UV} is usually assumed to be around $\sim M_{GUT}$.

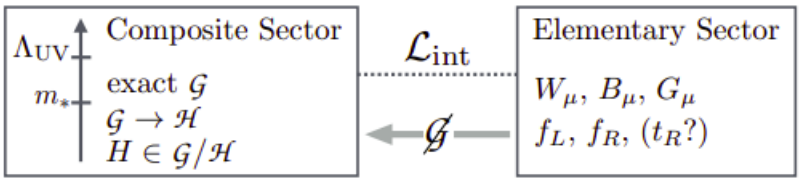

Figure 9: Brief scheme of the Composite Higgs framework [14].

3.2.3 Non-Minimal Composite Higgs model and searches for light scalars signals.

Among the vast ocean of different composite Higgs Models, we are interested in all them which can provide long-lived particle signatures. Some well-motivated models are related to Non-Minimal Composite Higgs[8]. These models take the coset $SO(7)/SO(6)$ to generate the Higgs as a pNGB[9]. These models are the context where heavy vector bosons and new light scalars, separated by a large mass gap, come out more naturally [19]. As mentioned in the quoted paper, interesting signals can be searched for at LHCb. Such signals come from rare $\mathcal{B}$ decays where light scalars and heavy vector bosons arise from the broken and unbroken generators and their couplings from the coset mentioned. Some of the most interesting channels are $B_s^0 \longrightarrow a_1 a_2$ and $B^+ \longrightarrow K^+ a_2 a_1$ with several muons in the final state. The Feynman diagrams for such processes can be seen in figure 10 where a heavy vector boson $\mathcal{V}$ is involved. The LLP particle might be the a_1. We consider the case where $m_{a_1} > 2m_{a_2}$.

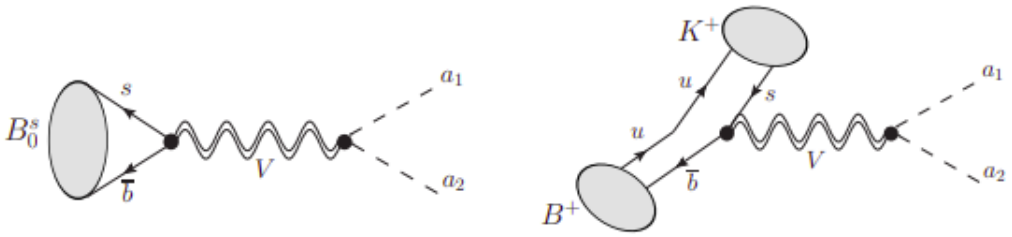

Figure 10: Tree level Feynman diagrams for the decays $B_s^0 \longrightarrow a_1 a_2$ (left) and $B^+ \longrightarrow K^+ a_2 a_1$ (right). Taken from [19].

For such processes, it would be really interesting to explore all these signatures which

[8]For a review of the minimal composite Higgs model, please check [14].
[9]For two concrete examples, see [17],[18].

lead to a_1 being in the LLP range. For such couplings, a Lagrangian term reads:

$$\mathcal{L} = \frac{1}{2}m_V^2 V_\mu V^\mu + \frac{1}{2}m_{a_1}^2 a_1^2 + \frac{1}{2}m_{a_2}^2 a_2^2 + m_{12}a_1^2 a_2 + V^\mu \left(g_{12}a_1\partial_\mu a_2 + g_{qq}(\bar{q}_L\gamma_\mu q_L)\right) + ..., \tag{3.10}$$

Notice the fact that the light scalars couple to leptons, following [19]. The decay width for such processes reads:

$$\Gamma(a_1 \longrightarrow l^+l^-) = \frac{g_1^2 y_l^2}{8\pi} m_{a_1}\left(1 - \frac{4m_l^2}{m_{a_1}^2}\right)^{3/2}, \tag{3.11}$$

In this work we will focus on this channel among others. If we assume that the main decay is into muons, we can easily get the value for our decay width:

$$\Gamma(a_1 \longrightarrow \mu^+\mu^-) = \frac{1}{\tau_{a_1}}, \tag{3.12}$$

and this is the equation we will use in order to obtain the coupling constant g_1.

3.3 Hidden Valleys.

3.3.1 General features of confining Hidden Valley scenarios.

We present in this section other promising models which can give rise to LLP signatures. Such models are the so-called Hidden Valleys (HVs) or Confining Hidden Valleys. They are principally based on a confining gauge group which is added to the standard model [20]. HVs are a class of models where there are relatively light states coupling to Standard Model (SM) states only via a heavy mediator [6]. This fact provides an amount of LLP states which can be studied at LHC and in particularly in the LHCb. Notice the vast amount of such models we can find in the literature. In this work we will be highly focused on all those which give rise to LLP signatures potentially detectable by LHCb. In the quoted reference [20] we can find a simple 'v-Model' which can reach this conditions. Actually this type of framework might give rise to the so-called 'emerging jets' signals where dark hadrons for instance are involved.

3.3.2 A simple confining 'v-Model'.

In this model we assume the addition of a non-abelian gauge group, let's say G_v to the SM gauge group, let's call it G_{SM}. At first, the SM particles are neutral under G_v, but on the other hand we have new light particles charged under G_v and neutral under

G_{SM}. The idea is that such new light particles (also called 'v-particles') can decay into SM particles via higher dimension operators. In the specific case of a confining hidden valley theory these particles are the 'v-hadrons'. The higher dimension operators (i.e. Z') comes out at TeV scale and can produce the decaying of long-lived 'v-hadrons'. A model of such type might be the one where a gauge group $U(1) \times SU(n_v)$ is added to the SM. The coupling constants for both gauge groups are g' and g_v respectively. The idea is that $SU(n_v)$ is capable of providing an interaction which confines at the scale $\Lambda_v \sim$TeV. The $U(1)$ can be broken giving a massive boson Z'. To finish the model we add two v-quarks flavours $U, \bar{U}$ and $C, \bar{C}$ in the n_v and $\bar{n}_v$ representations together with N_i right-handed neutrinos. Of course the breakdown of $U(1)$ comes from the acquisition of a non-zero expectation value by $\langle\phi\rangle$ which also provides the masses to all those particles above mentioned. The lagrangian content for the gauge boson Z_μ could be in such a way [21]:

$$\mathcal{L} = g_v Z^\mu (Q_v^{SM} \bar{q}\gamma_\mu q + Q_v^{HV} \bar{q}_v \gamma_\mu q_v) + \frac{1}{2} m_Z^2 Z^2 + ..., \tag{3.13}$$

where the hierarchy for the charges reads $Q_v^{SM} \ll Q_v^{HV}$ coming the SM coupling from kinetic mixing [22]. In this way, the Z^μ meanly decays to the hidden sector. Here the q are the usual right-handed SM quarks and the same for q_v but for the hidden sector. The charge assignments under the different gauge groups is presented in figure 11. A

	q_i	$\bar{u}_i$	$\bar{d}_i$	ℓ_i	e_i^+	N_i	U	$\bar{U}$	C	$\bar{C}$	H	ϕ
$SU(3)$	**3**	$\overline{\mathbf{3}}$	$\overline{\mathbf{3}}$	**1**	**1**	**1**	**1**	**1**	**1**	**1**	**1**	**1**
$SU(2)$	**2**	**1**	**1**	**2**	**1**	**1**	**1**	**1**	**1**	**1**	**2**	**1**
$U(1)_Y$	$\frac{1}{6}$	$-\frac{2}{3}$	$\frac{1}{3}$	$-\frac{1}{2}$	1	0	0	0	0	0	$\frac{1}{2}$	0
$U(1)_\chi$	$-\frac{1}{5}$	$-\frac{1}{5}$	$\frac{3}{5}$	$\frac{3}{5}$	$-\frac{1}{5}$	-1	q_+	q_-	$-q_+$	$-q_-$	$\frac{2}{5}$	2
$SU(n_v)$	**1**	**1**	**1**	**1**	**1**	**1**	$\mathbf{n_v}$	$\overline{\mathbf{n_v}}$	$\mathbf{n_v}$	$\overline{\mathbf{n_v}}$	**1**	**1**

Figure 11: Charge assignments for the model.

$\mathcal{Z}_2$ symmetry is also imposed forbidding Dirac neutrino masses. On the other hand, a mixing between U(1) and hypercharge of the type $\frac{1}{2} k F'_{\mu\nu} F_Y^{\mu\nu}$, but k can be removed with field redefinitions in terms of the charges [20].

Now we consider the case $m_U \sim m_C \ll \Lambda_v$. In this regime is acceptable to think about a v-isospin with U and C which by analogy we can name it 'v-pions' π_v^0, π_v^0. In the specific case of the neutral state, with a v-quark wave function such that $U\bar{U} - C\bar{C}$ we can explore the channels either $U\bar{U} \longrightarrow Z' \longrightarrow f\bar{f}$ or $C\bar{C} \longrightarrow Z' \longrightarrow f\bar{f}$. In this

way, the total decay width reads

$$\Gamma = \frac{1}{8\pi}\frac{g'^4}{m_Z'^4}\frac{Q_\phi^2 Q_H^2 f_{\pi_v^2} m_{\pi_v}^5}{(m_{\pi_v}^2 - m_Z^2)^2}\sum N_c^f m_f^2 v_f, \tag{3.14}$$

where m_f, v_f make reference to the fermion mass and velocity. The term N_c takes the values 3 for quarks and 1 for leptons. It is an usual result when we work in the regime far away from $m_{\pi_v \sim m_Z}$. Other cases can be explored such as

$$\Gamma_{\pi_v \longrightarrow b\bar{b}} \sim 3 \times 10^{15} \mathrm{s}^{-1} \frac{f_{\pi_{nu}}^2 m_{\pi_v}}{(200\ \mathrm{GeV})^3}\left(\frac{10\ \mathrm{TeV}}{m_Z/g'}\right), \tag{3.15}$$

when we work in the regime $2m_b < m_{\pi_v} < 2m_t$. On the other hand, for $m_{\pi_v} \ll m_Z$:

$$\Gamma_{\pi_v \longrightarrow b\bar{b}} \sim 6 \times 10^{9} \mathrm{s}^{-1} \frac{f_{\pi_{nu}}^2 m_{\pi_v}^5}{(20\ \mathrm{GeV})^7}\left(\frac{10\ \mathrm{TeV}}{m_Z/g'}\right). \tag{3.16}$$

The specific numbers shown come from taking $n_v = 3$, $k = 0$ and $q_+ = -2$ as is done in the original work [23]. The pion will decay either prompt or by means of a displaced vertex. The above 'v-Model' is usually called as the 'Two light Flavour' model and it is supposed to give signals as the one shown in figure 12. This kind

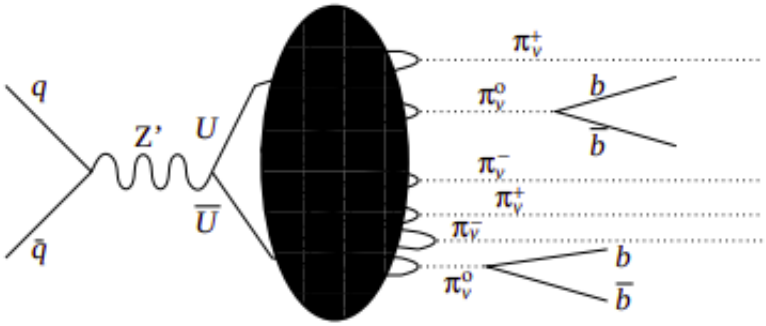

Figure 12: A possible event in the Two Light Flavour Case. Taken from [20].

of model goes inside a general framework called 'Heavy flavour channels', however, there are others type of models which can also give rise to signatures where muon pairs arise in the final state. The so-called 'dimuon channel' is also explored in [21] which comes out also as another important channel to search for at LHCb.

3.3.3 Hidden Valley models with a complex scalar particle as a mediator. Emerging jets signatures.

Now we follow a more recent work [24] which develops an specific study about the 'emerging jets' mentioned before. This paper explore the specific example of $n_v = 3$

and uses a complex scalar field X_d as a mediator instead of the vector boson as before. Namely, we add a *dark QCD* to the SM. In fact X_d is bifundamental under both QCD and dark color and the typical extension here would be $G_{SM} \times S(U)_{n_v}$ [25]. In this way, the only allowed Yukawa type coupling is of the form

$$\mathcal{L}_\kappa = \kappa_{ij} \bar{Q}_{d_i} q_j X'_d + h.c, \tag{3.17}$$

being q_j the usual right-handed SM quarks and κ the $n_f \times 3$ matrix of Yukawa couplings. To summarize, the complete lagrangian at high scales for this model reads

$$\mathcal{L} = \bar{Q}_{d_i}(\not{D} - m_d) Q_{d_i} + (D_\mu X_d)(D^\mu X_d)^\dagger - M_d^2 X_d X_d^\dagger - \frac{1}{4} G_d^{\mu\nu} G_{\mu\nu,d} + \mathcal{L}_d + \mathcal{L}_{SM}, \tag{3.18}$$

where $G_d^{\mu\nu}$ is the dark gluon field strength tensor. Figure 13 shows an scheme of the charge content for the fields. As mentioned before, this model also provides pion

Field	$SU(3) \times SU(2) \times U(1)$	$SU(3)_{\text{dark}}$	Mass	Spin
Q_d	$(1, 1, 0)$	(3)	m_d $\mathcal{O}$(GeV)	Dirac Fermion
X_d	$(3, 1, \frac{1}{3})$	(3)	M_{X_d} $\mathcal{O}$(TeV)	Complex Scalar

Figure 13: Charge content for the different relevant fields in the Hidden Valley model.

states in such a way π_d. The relevant effective lagrangian term when the mediator X_d is integrated out[10] reads

$$\mathcal{L}_{eff} \sim m_{ij} \bar{Q}_{L_i} Q_{R_j} + \kappa_{i\alpha} \kappa^*_{j\beta} \frac{1}{M_X^2} \bar{Q}_{L_i} \gamma_\mu Q_{R_j} \bar{d}_{R_\alpha} \gamma^\mu d_{R_\beta} + h.c. \tag{3.19}$$

These terms give rise to decay width like

$$\Gamma(\pi_d \longrightarrow \bar{d}d) = \frac{\kappa^4 N_c f_{\pi_d^2} m^2_{down}}{32\pi M_{X_d^4}} m_{\pi_d}. \tag{3.20}$$

Notice that this equation holds for all down quark types, which means is also relevant for bottom quarks, highly motivated in LHCb searches. Finally, we give an estimation of the decay length involving such decay width:

$$c\tau_0 \approx 80 \text{ mm} \times \frac{1}{\kappa^4} \times \left(\frac{2 \text{ GeV}}{f_{\pi_d}}\right)^2 \left(\frac{100 \text{ MeV}}{m_{down}}\right)^2 \left(\frac{2\text{GeV}}{m_{\pi_d}}\right) \left(\frac{M_{X_d}}{11 \text{ TeV}}\right)^4, \tag{3.21}$$

so we could say it is well motivated to consider centimeter to meter decay lengths for GeV scale dark pions with TeV scale mediators. On the other hand, specifically

[10]For a better comprehension of the concept 'integrating out' heavy field, please see [26].

speaking about the LHCb detector, it can be competitive looking for such signals whether dark quark pairs are produced at LHC. These events wold be produced by lagragian terms as

$$\mathcal{L} \sim \frac{1}{\Lambda^2}(\bar{q}\Gamma_q q)(\bar{Q}_d\Gamma_d Q_d), \tag{3.22}$$

where effective operators arise again. Γ is understood as Dirac structures. So in this way our aim would be search for dark pions coming from these $\bar{Q}_d Q_d$ events. Two models are researched by the reference paper. Both provide encouraging event rate of the dark pions.

3.4 SUSY models with R-parity violation.

The supersymmetric (SUSY) models are highly well-motivated among all the theoretical literature related to physics BSM. Some of these models present several solutions to SM problems which actually can have the SM. In this work we briefly discuss two of these models; the simplest one, the Minimal Supersymmetric Standard Model (MSSM) and an extension of it, taking into account the so-called supersymmetric models with R-parity violation.

3.4.1 A brief review about SUSYs theories.

In order to build up theories which involve supersymmetry, we must first try to understand the framework. SUSY is introduced as a symmetry capable of relating boson and fermions to each other. Namely, the operator Q acts as follows:

$$Q\,|fermion\rangle = |boson\rangle\,, \tag{3.23}$$

and viceversa. In a SUSY theory, particles are assigned to chiral supermultiplets (also called superfields) and to vector supermultiplets [27]. In the MSSM the full particle spectrum is shown in figure 14. Notice that all those spartners[11] are denoted by a tilde. The main aim of imposing such symmetry is to get the fermion/boson version of the particles of the SM. This will provide us some solutions to problems like *Hierarchy*. Finally, we must point out that two Higgs appear in this model. This is required of keep the theory anomaly-free and to provide masses to all the particles, even the spartners. This fact will be achieved making use of the superpotential W. On the other hand, in order to complete the full MSSM particle content, the SM gauge fields

[11]The members of one supermultiplet are called superpartners (or short: spartners)

Names		spin 0	spin 1/2	$SU(3)_C$, $SU(2)_L$, $U(1)_Y$
squarks, quarks	Q	$(\widetilde{u}_L \;\; \widetilde{d}_L)$	$(u_L \;\; d_L)$	$(\mathbf{3}, \mathbf{2}, \frac{1}{6})$
(×3 families)	$\overline{u}$	$\widetilde{u}^*_R$	$u^\dagger_R$	$(\overline{\mathbf{3}}, \mathbf{1}, -\frac{2}{3})$
	$\overline{d}$	$\widetilde{d}^*_R$	$d^\dagger_R$	$(\overline{\mathbf{3}}, \mathbf{1}, \frac{1}{3})$
sleptons, leptons	L	$(\widetilde{\nu} \;\; \widetilde{e}_L)$	$(\nu \;\; e_L)$	$(\mathbf{1}, \mathbf{2}, -\frac{1}{2})$
(×3 families)	$\overline{e}$	$\widetilde{e}^*_R$	$e^\dagger_R$	$(\mathbf{1}, \mathbf{1}, 1)$
Higgs, higgsinos	H_u	$(H^+_u \;\; H^0_u)$	$(\widetilde{H}^+_u \;\; \widetilde{H}^0_u)$	$(\mathbf{1}, \mathbf{2}, +\frac{1}{2})$
	H_d	$(H^0_d \;\; H^-_d)$	$(\widetilde{H}^0_d \;\; \widetilde{H}^-_d)$	$(\mathbf{1}, \mathbf{2}, -\frac{1}{2})$

Figure 14: Particle content of the MSSM.

are associated with vector supermultiplets[12] in the MSSM, as shown in figure 15. The

Names	spin 1/2	spin 1	$SU(3)_C$, $SU(2)_L$, $U(1)_Y$
gluino, gluon	$\widetilde{g}$	g	$(\mathbf{8}, \mathbf{1}, 0)$
winos, W bosons	$\widetilde{W}^\pm \;\; \widetilde{W}^0$	$W^\pm \;\; W^0$	$(\mathbf{1}, \mathbf{3}, 0)$
bino, B boson	$\widetilde{B}^0$	B^0	$(\mathbf{1}, \mathbf{1}, 0)$

Figure 15: Complete set of Gauge fields in MSSM.

usual parametrization of a chiral supermultiplet is:

$$\Phi = \phi(y) + \sqrt{2}\theta\psi(y) + \theta\theta F(y), \tag{3.24}$$

where y^μ and θ are superspace coordinates[13]. Therefore a chiral supermultiplet is a function of a scalar field ϕ, a fermionic field ψ and an auxiliary boson field F. The parametrization for a vector supermultiplet reads (in Wess-Zumino gauge):

$$V = \theta^\dagger\bar{\sigma}^\mu\theta A_\mu + \theta^\dagger\theta^\dagger\theta\lambda + \theta\theta\theta^\dagger\lambda^\dagger + \frac{1}{2}\theta\theta\theta^\dagger\theta^\dagger D, \tag{3.25}$$

[12]The spartners of quarks are squarks, for leptons are sleptons, for Higgs higgsinos and for gauge fields gauginos, i.e. the SUSY partners of the gluons are gluinos, for W bosons are winos and for the hypercharge boson B_μ is a bino.

[13]Notice that a superspace also contains four fermionic coordinates, which have the properties of the usual Grassmmann variables.

being A_μ the vector boson λ the gaugino and D the auxiliary boson field as well as F. The tipical lagrangian term for such theory reads:

$$\mathcal{L} = \left(K(\Phi_i, \tilde{\Phi}^{\star j})\right)_D + \left(\left(\frac{1}{4} f_{ab}(\Phi_i)\hat{\mathcal{W}}^{a\alpha}\hat{\mathcal{W}}^b_\alpha + W(\Phi_i)\right)_F + c.c\right), \tag{3.26}$$

where three main terms are involved. The first term is the so-called Käler potential. It usually take the trivial form at tree level as

$$K = \Phi_i, \tilde{\Phi}^{\star j}, \tag{3.27}$$

where $\tilde{\Phi}^{\star j} = (\Phi^\star e^V)^j$ with $V = 2g_a T^a V^a$. Here g_a is the coupling constant and T^a the generators. The gauge kinetic function f_{ab}, can be expressed as:

$$f_{ab} = \delta_{ab}\left(\frac{1}{g_a^2} - i\frac{\Theta_a}{8\pi^2}\right), \tag{3.28}$$

Θ_a is a CP-violating parameter. The field strengths read

$$\hat{\mathcal{W}}^a_\alpha = g_a \mathcal{W}^a_\alpha = -\frac{1}{4}\bar{D}\bar{D}(D_\alpha \hat{V}^\alpha - i f^{abc}\hat{V}^b D_\alpha \hat{V}^c + ...), \tag{3.29}$$

and last but not least, the superpotential W. This is actually one of the most important pieces of the SUSY lagrangian and we will discuss it in detail. The most generic form is [27][14].

$$W = L^i\Phi_i + \frac{1}{2}M^{ij}\Phi_i\Phi_j + \frac{1}{6}y^{ijk}\Phi_i\Phi_j\Phi_k. \tag{3.30}$$

With this amount of information, the vertices for such SUSY theory (which come from W superpotential) are the ones shown in figures 16 and 17. Notice that the ones in figure 16 are needed in order to manage the quadratic correction to the Higgs mass and therefore solve the hierarchy problem[15]. Finally, since we need a well-motivated phenomenological theory, we need SUSY to be broken at some energy scale. This breaking is usually called 'soft' since we need terms which do not involve quadratic divergences in quantum corrections to scalar masses. The usual Lagrangian density that is invariant under supersymmetry, but not under a vacuum state, could be

$$\mathcal{L}_{soft} = -\left(\frac{1}{2}M_a\lambda^a\lambda^a + \frac{1}{6}a^{ijk}\phi_i\phi_j\phi_k + \frac{1}{2}b^{ij}\phi_i\phi_j + t^i\phi_i\right) + c.c. - (m^2)^i_j\phi^{\star j}\phi_i, \tag{3.31}$$

where the first term comprises the gaugino masses, the second and third terms are the so-called A-term and B-term involving scalar components of three and two chiral

[14]Notice that the W potential only depends on the scalar components of the chiral superfields.

[15]We also have the gauge couplings of the SUSY theory, but we are not interested in them so far, for further information see [27].

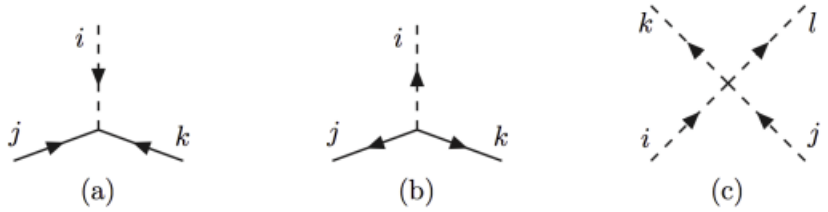

Figure 16: The dimensionless non-gauge interaction vertices in a supersymmetric theory: (a) scalar-fermion-fermion Yukawa interaction y^{ijk}, (b) the complex conjugate interaction y^*_{ijk}, and (c) quartic scalar interaction $y^{ijn}y^*_{kln}$.

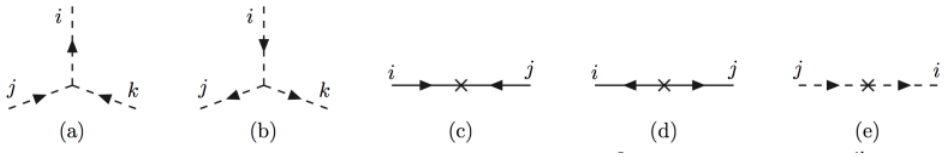

Figure 17: Supersymmetric dimensionful couplings: (a) (scalar)^3 interaction vertex $M^*_{in}y^{jkn}$ and (b) the conjugate interaction $M^{in}y^*_{jkn}$, (c) fermion mass term M^{ij} and (d) conjugate fermion mass term M^*_{ij} , and (e) scalar squared-mass term $M^*_{ik}M_{kj}$.

superfields, respectively, the fourth term, if existing, is the tadpole term and the last term is related to the soft masses of the scalar components of the chiral superfields. There are also two more terms which can appear, a term which can be 'maybe soft' and another one related to spinors components of the superfields. These read:

$$\mathcal{L}_{maybe\ \ soft} = -\frac{1}{2}c_i^{jk}\phi^{\star i}\phi_j\phi_k + c.c., \tag{3.32}$$

$$\mathcal{L} = -M^a_{Dirac}\lambda^a\psi_a + c.c. \tag{3.33}$$

The last term is only available if chiral superfield transforms under the adjoint representation of the gauge group(s). This is not the case for MSSM, explained in the following.

3.4.2 The Minimal Supersymmetric Standard Model (MSSM).

Regarding the specific MSSM case, the W superpotential would take the form:

$$W_{MSSM} = \bar{u}y_uQH_u - \bar{d}y_dQH_d - \bar{e}y_eLH_d + \mu H_uH_d. \tag{3.34}$$

These terms are not the only allowed at renomarlization level. Some terms may appear to explicitly break lepton and baryon number symmetries. In order to get over

this problem, the R-parity symmetry (also called matter parity) is usually demanded. The eigenvalues for such symmetry are

$$P_R = (-1)^{3(B-L)+2s}. \tag{3.35}$$

Notice that no theoretical motivations encourage such symmetry but rather experimental constrains such as the non observation of a proton decay. The SM particles have R-parity eigenvalue +1 and all those new particles from SUSY have -1. From this point of view this symmetry provide a difference between SM-like particles and SUSY-like ones. Finally, the complete soft SUSY breaking Lagrangian reads

$$\begin{aligned}
\mathcal{L}_{soft}^{MSSM} = &-\frac{1}{2}\left(M_3\tilde{g}\tilde{g} + M_2\tilde{W}\tilde{W} + M_1\tilde{B}\tilde{B} + c.c\right) - \\
&- \left(\tilde{\bar{u}}a_u\tilde{Q}H_u + \tilde{\bar{d}}a_d\tilde{Q}H_d + \tilde{\bar{e}}a_e\tilde{Q}H_d + c.c.\right) - \\
&- \tilde{Q}^\dagger m_Q^2\tilde{Q} - \tilde{L}^\dagger m_L^2\tilde{L} - \tilde{u}m_u^2\tilde{u}^\dagger - \tilde{\bar{d}}m_d^2\tilde{\bar{d}}^\dagger - \tilde{\bar{e}}m_e^2\tilde{\bar{e}}^\dagger - \\
&- m_{H_u}^2 H_u^\star H_u - m_{H_d}^2 H_d^\star H_d - (bH_uH_d + c.c),
\end{aligned} \tag{3.36}$$

where the mases for the gauginos come out in the first term together with the so-called A-terms in the second line. The third line and part of the fourth one show the soft masses related to both superfields and higgs doublets respectively and the last term is the so-called B-μ term related to the μ-term which appears in the W potential. All the incoming parameters are supposed to be around the mass scale $\sim m_{soft} \sim$ TeV. Notice that here the breakdown of SUSY is carried out by means of explicit lagrangian terms which achieve this goal, but it is not an usual way to procedure. Usually we are going to demand an spontaneous symmetry breaking by means of other methods. The so-called D-term and F-term[16] are used in order to break such symmetry.

3.4.3 The R-parity violation SUSY models.

From the last part of the discussion in the last paragraph we have found out that it is better to make the break of SUSY by means of other methods. This breakdown occurs in a hidden sector which practically does not interact with the visible sector (MSSM) but rather both sectors do share some interactions that are responsible for mediating supersymmetry breaking from the hidden sector to the visible sector, resulting in the MSSM soft terms. There are several ways of breaking SUSY and also transferring this breaking to the visible sector. Some of them give rise to LLP signatures [28]. We focus here in a well-motivated mechanism as R-parity violation. As it

[16]Such terms come from the D and F fields used in SUSY in order to have a well degrees of freedom counting for fermion and boson, $n_F = n_B$, in the on-shell and off-shell cases.

was mentioned before, no theoretical requirements demand such symmetry. It is possible thus to explore a more generic R-parity breaking inside a global theory beyond MSSM. The most general renormalizable Lagrangian with RPV operators contains a W superpotential like

$$\mathcal{W}_{RPV} = \mu_i L_i H_u + \frac{1}{2}\lambda_{ijk} L_i L_j \bar{e}_k + \lambda'_{ijk} L_i Q_j \bar{d}_k + \frac{1}{2}\lambda''_{ijk} \bar{u}_i \bar{d}_j \bar{d}_j. \tag{3.37}$$

Notice that this is a general expression, there are models in which only some terms are taken into account such as bilinear R-parity models [29]. Even more, we can have models of dynamical R-parity [28] which we have not developed here. The RPV coefficients must be small as they are highly constrained from flavor measurements and non-observation of the proton decay. This fact turns out to be crucial in order to have LLP signatures. One of these can be the Lightest Supersymmetric Particle (LSP). The inverse decay width for the neutralino decaying off-shell into a lepton a two quarks read:

$$\Gamma^{-1}(\tilde{\chi}_0 \longrightarrow l_i q_j q_k) \sim \left(\frac{m_{\tilde{l}_i}}{750\ \text{GeV}}\right)^4 \left(\frac{100\ \text{GeV}}{m_{\tilde{\chi}_0}}\right)^5 \left(\frac{10 \times 10^{-5}\ \text{GeV}}{\lambda'_{ijk}}\right)^2 \times 0.1\ \text{ns}. \tag{3.38}$$

Other interesting models can be pointed out in order to give rise to different signatures like neutralinos decaying to $e^{\pm}\mu^{\pm}\nu$ [8] being the neutralino the LLP. Others signals may come from the so-called minimal supergravity model with bilinear R-parity violation (mSUGRA) [30] which gives rise to this type of channels[17].

4 Experimental Status.

We have given an extended overview about theoretical models involving LLPs searches. Now in this section our aim is to look at the current experimental situation. We focus on the specific channels where LLPs are very motivated to be found at LHCb. We will also discuss some experimental constrains and show sensibility plots made by other collaborations.

4.1 Searching for low-mass dimuon resonances.

Some of the most relevant searches inside the LHCb collaboration are the ones in which one has muons in the final state. These searches are highly motivated for

[17]For more allowed channels provided by mSUGRA theory, please check [23].

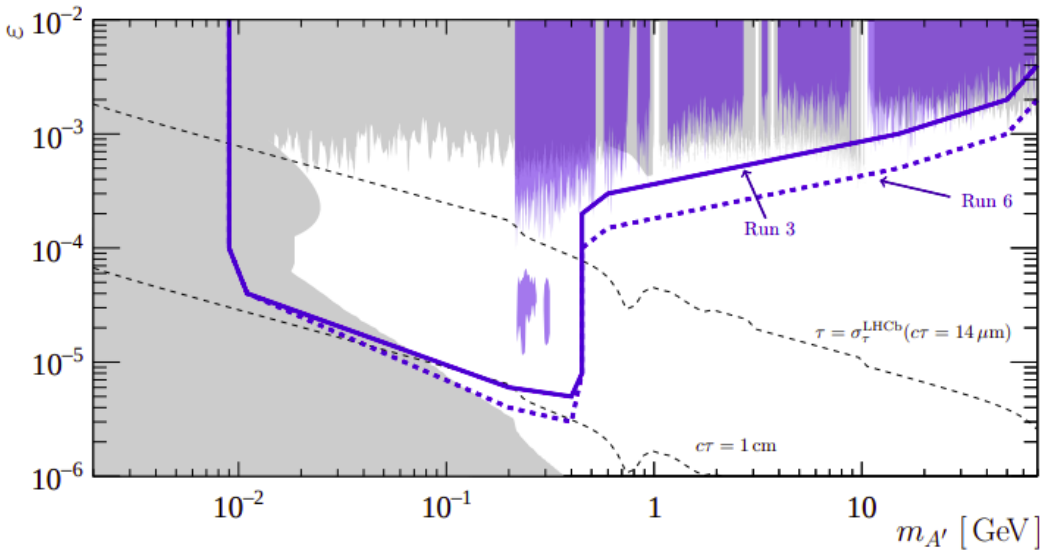

Figure 18: Experimental constraints on visible Dark Photon decays (blue regions) at LHCb. The solid blue line is the union of Run III projections for LHCb together with inclusive $A' \to e^+e^-$ projections enabled by recent advances in the LHCb trigger [11].

models where a dark boson appears (in our specific case for the Dark Photon) or when intermediate light scalars arise (specifically studied in this work), as explained in section 3. Recent works in this topic set up the most recent experimental constrains together with the new projections in LHCb Run III as it is shown in figure 18. On the other hand, specific searches have been carried out at LHCb for more general models where a general X boson is involved [7]. In the cited paper, low-mass dimuon resonances are searched. They were produced in pp collisions at a center-of-mass energy of 13 TeV, using a data sample corresponding to an integrated luminosity of 5.1 fb^{-1} collected with the LHCb detector in 2016–2018. The X bosons can either decay promptly or displaced from the proton-proton collision. For both situations we have different channels to explore, either inclusive or exclusive ($X + b$ for prompt decays, and X required to decay promptly after pp collision for displaced vertices). No relevant signals have been found.

4.2 Searching for LLPs decaying to $e^{\pm}\mu^{\pm}\nu$.

Other well-motivated signals to look for at LHCb are those ones where in the final states three specific particles arise: an electron/positron together with an antimuon/muon and a neutrino. The most enthusiastic theoretical framework which supports such decays might be the SUSY models with R-parity violation, explained in

section 3, and also those ones where a right-handed neutrino is considered. Usually the LLP particle is the neutralino χ_0^1. The first direct search of such channel at LHCb can be found in reference [8]. The exploration of these channels were made with pp collision at $\sqrt{s} = 13$ TeV and a total integrated luminosity of $5.38 \pm 0.11 \text{fb}^{-1}$. The search covers LLP masses from 7 to 50 GeV/c^2, lifetimes from 2 to 50 ps and considers three production mechanisms: the direct pair production (DPP) from the interaction of quarks, the pair production from the decay of a SM-like Higgs boson (HIG) with a mass of 125 GeV/c^2, and the charged current production from an on-shell W boson (CC) with an additional lepton. No signal is reported by the collaboration. The results are in agreement with the only-background hypothesis. Nevertheless, some upper limits at 95% confidence level are made for the cross section times the branching ratios for the three processes. In the case of DPP mechanism, justified by SUSY-R framework, the study was done fixing initially the mass of the neutralino and fixing the lifetime of it later on as is shown in figure 19. For the others channels some upper

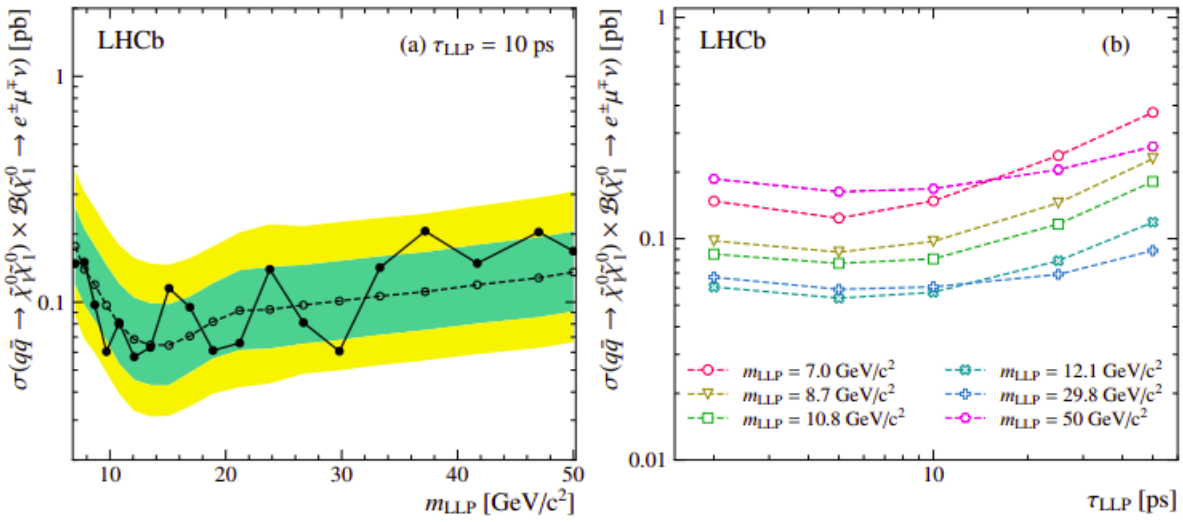

Figure 19: Expected (open circles and dotted line) and observed (filled circles and solid line) upper limits of the cross-section as a function of m_{LLP} for $\tau_{LLP} = 10$ ps. The green and yellow bands indicate the quantiles of the expected upper limit corresponding to $\pm 1\sigma$ and $\pm 2\sigma$ for a Gaussian distribution. Observed limits on the cross-section as a function of τ_{LLP} for different m_{LPP} values for LLPs produced through the DPP mechanism.

limits are also made but fixing the mass to the lowest one, 7 GeV/c^2, and the one which shows the best fit, 29.8 GeV/c^2 [8]. Since they do not provide further relevant information, they are not presented in this work.

4.3 Searching for emerging jets.

Another recent search carried out by LHCb is related to emerging jets. These searches can be found in the context (among the vast literature) of HV or SUSY-R models [7]. Even for Dark Photon model if a Dark Photon together with jets are considered in the event. In this section we mainly mention the most recent work [31]. This is motivated to the search of light dark states coming from SM-like Higgs decays. The data sample analysed corresponds to 0.62 fb^{-1} at a centre-of-mass energy of $\sqrt{s} = 7$ TeV and 1.38 fb^{-1} at $\sqrt{s} = 8$ TeV. The search is made in the ranges of lifetimes from 2 to 500 ps and with a LLP mass from 25 to 50 GeV/c^2. Again no signals are encountered and upper limits to the cross section times branching ratios are made as shown in figure 20. The decays taken into account are to $b\bar{b}$, $c\bar{c}$ and $s\bar{s}$.

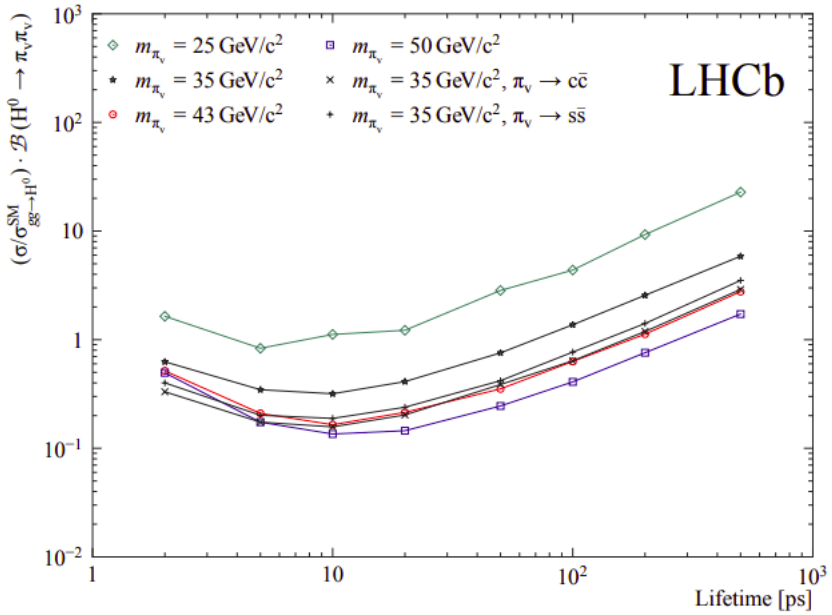

Figure 20: Observed upper limit versus lifetime for different π_d masses and decay modes. In general the decay to $b\bar{b}$ is assumed, otherwise is specified.

5 Study of some models concerning LLPs signatures.

In this section we present the results obtained from the analysis of the LHCb simulations both in the case of the Dark Boson model and the Composite Higgs model. The Dark Boson Model was already studied in a previous work [4], here we present just the main results. The Composite Higgs Model has been specifically studied in

this work. The simulations in both cases were carried out using the LHCb Software. The idea of the study has been to obtain some information about how much tracks we are missing with the current trigger. For this, a complete study of the displaced vertices proportions has been carried out. The displaced vertices together with the different tracks types were explained in section 2. The samples were generated using Pythia8 and assuming Run 3 beam conditions. The $B \rightarrow H'(\rightarrow \mu^+\mu^-)K$ decay channel was generated for the study of the Dark Higgs Model. In an analogous way, the $B^+ \rightarrow K^+a_1(\rightarrow \mu^+\mu^-)a_2(\mu^+\mu^-)$ decay channel was generated for the study of the Composite Higgs Model.

5.1 Study of the Dark Boson Model.

Before developing the main model studied in this work, we briefly revise a previous work where the efficiency of HLT1 trigger stage on LLPs was performed [4].The studied model is based on a gauge singlet Higgs field weakly mixing with the SM higgs field. In this way this new Higgs plays the role of a mediator between the SM and a hidden sector. This phenomenology is analogous to the one already shown in the Dark Photon Model even though the physics is slightly different. The mixing comes from the expression

$$h = Hcos\theta - H_0 sin\theta, \tag{5.1}$$

where h is the resulting state of the mixing and H the SM 125 GeV/c^2 Higgs boson together with H_0, an additional state of unknown mass. Two signatures were investigated: $B^+ \rightarrow K^+H_0(\rightarrow \mu^+\mu^-)$ and $B^0 \rightarrow K^*(894)H_0(\rightarrow \mu^+\mu^-)$. An amount of 55 Monte Carlo (MC) samples of 7000 events were generated with Higgs variables:

- Lifetime τ = 100 ps and mass M from 500 to 4500 MeV/c^2, by 500 MeV/c^2 steps.
- Mass M = 2500 MeV/c^2 and lifetime τ = 1, 10, 100 and 1000 ps.

This work was motivated by a previous one [32] which indeed studied the sensibility of different experiments for these channels, as it shown in figure 21. Vertex proportions were obtained at reconstructive level for the parameters $sin\theta$ and dark Higgs mass as well as TOS on this dark Higgs. In figures 22, 23 and 24 this is shown. From the pictures we can see a relevant region between 1 and 10 ps for LL vertices meanwhile the relevant one for DD and also for TT is between 100 ps and 500 ps. At this point, this study help us understanding the projected performance of the first stage of the LHCb trigger system (HLT1) when reconstructing LLPs. And in this way we

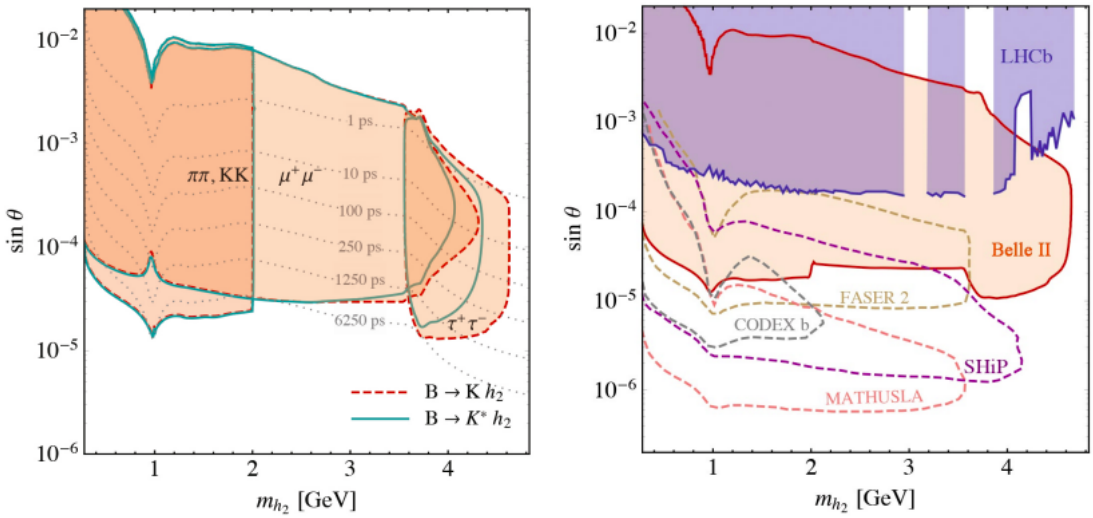

Figure 21: (Left) Parameters regions for three or more events for the channel $B \to Kh_2(\to f)$ with $f = \pi\pi + KK\ \mu^+\ \mu^-\ \tau^+\ \tau^-$, for Belle II experiment. (Right) Sensitibity of the Belle II experiment for the channels $B \to Kh_2$, $B \to K^*h_2$ and also for decay channels of h_2 to $f = \pi\pi + KK\ \mu^+\ \mu^-\ \tau^+\ \tau^-$, this case is specifically focused on displaced vertices of h_2.

can investigate the efficiency of other promising models as the one presented in the next section.

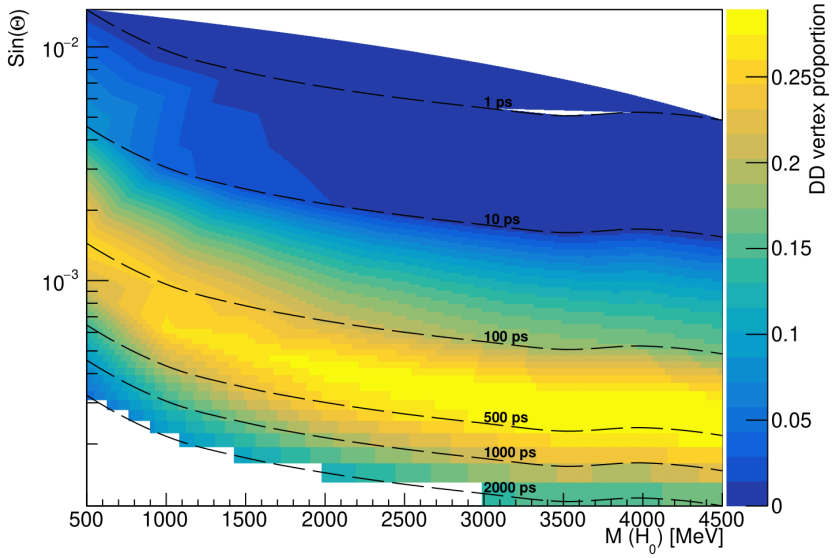

Figure 23: Vertex proportion at reconstructive level for DD displaced vertices as a function of the mass of the Dark Higgs and the mixing parameter $sin\theta$ in the case of Dark Boson Model.

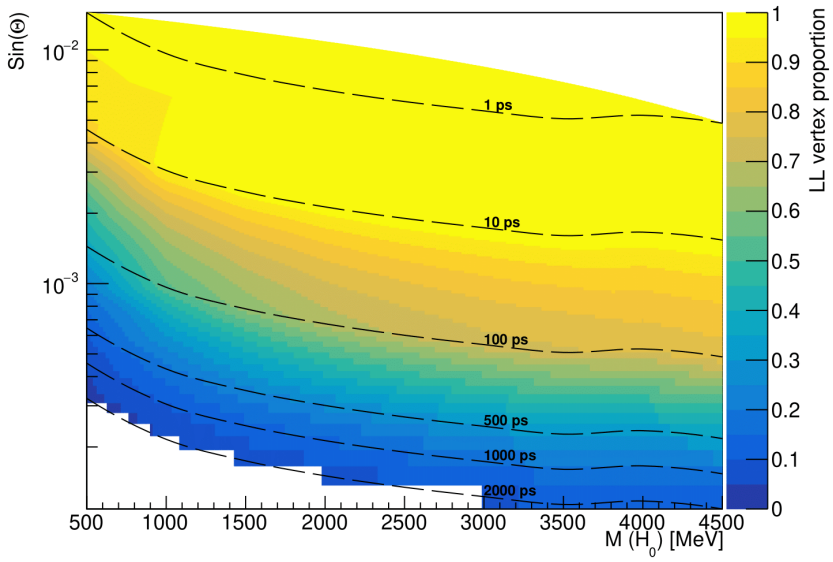

Figure 22: Vertex proportion at reconstructive level for LL displaced vertices as a function of the mass of the Dark Higgs and the mixing parameter $sin\theta$ in the case of Dark Boson Model.

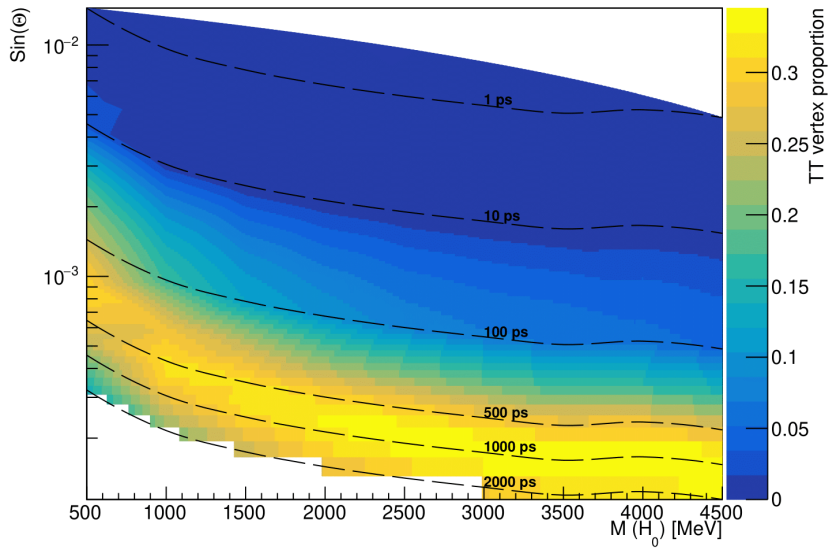

Figure 24: Vertex proportion at reconstructive level for TT displaced vertices as a function of the mass of the Dark Higgs and the mixing parameter $sin\theta$ in the case of Dark Boson Model.

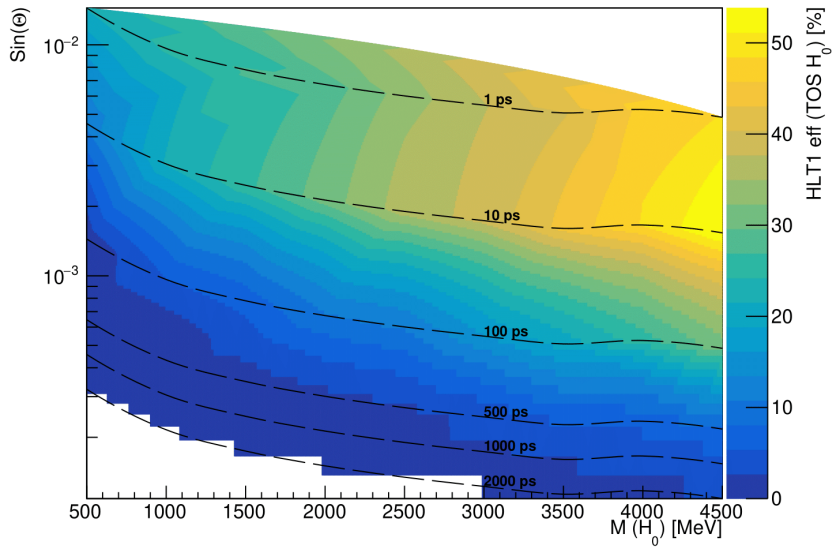

Figure 25: Proportion of events where the HLT1 triggers on a child of the dark Higgs.

These figures show how the displaced vertices distributions are plotted in the parameters space considering this model. The figures where displaced vertices distributions are plotted give us an overview about the capability of reconstructing the different tracks coming from the Long-lived Higgs. In Fig. 25 is presented one of the different lines which contributes to the total HLT1 efficiency, as it was mentioned in sec. 2. This plots highlights the fact that an improvement in the HLT1 trigger stage is needed in order to increase the trigger efficiency to Long-Lived particles. This fact will also be pointed out in the next section.

5.2 Study of the Composite Higgs model involving light scalars signatures.

In order to develop an specific case, we study the situation where we have light states provided by Composite Higgs scenarios coming from rare B decays. The channel under study is $B^+ \to K^+ a_1(\to \mu^+\mu^-)a_2(\mu^+\mu^-)$. One of this light scalar is assumed to be Long-Lived. The full simulation consists of 44 MC samples of 1000 events whose variables were:

- Masses from M=500 MeV/c^2 to 2000 MeV/c^2 in steps of 500 MeV/c^2 and lifetime τ=1,10,100,250,500,750,1000,1250,1500,1750 and 2000 ps.

The results obtained were the following. In figure 26 we can see the transversal mo-

mentum distribution for different lifetimes and masses of the light scalar a_1, also we got the end decay vertex point in the z direction. These two plots give us some context to understand the following information related to vertices proportions. The vertices proportions at reconstructive level[18] were performed both for lifetime vs masses and g_1 vs lifetimes. The g_1 is the coupling constant between the leptons and the light scalar supposed to be the Long-lived particle. This parameter is fixed with the decay width for a channel where only muons in the final state are allowed $\Gamma(a_1 \to \mu^+\mu^-)$ as it was shown in eq. 3.11. The distributions are shown in the figures 27, 28 and 29.

After showing the figures where displaced vertices are plotted in the parameter space, we can extract some conclusion. Firstly, we realise that the dependence of HLT1 on only Long tracks, can be negligible in the parameter's region where lifetimes are low, but we cannot say the same for the rest of the parameter space. We get in this model, and in the previous one, some vertices proportions which can be important specially for DD and TT displaced vertices. As we can see in figure 27, below 10 ps, LL are the most important displaced vertices, as we pointed out, but in the figures 28 and 29, we find some important propotions of DD and TT displaced vertices above the 10 ps. In this sense the HLT1 trigger stage will not be considering this kind of tracks, so this information will be missed. So we find an important conclusion, Downstream and T tracks (coming from DD and TT displaced vertices) are important enough to contribute to the HLT1 efficiency to find LLP. This is what it is shown in figure 30, which tells us that the proportions of LL+DD vertices missed can reach in some points of the parameter space around 60%.

[18]Reconstructive level means we take into account the interaction with the detector.

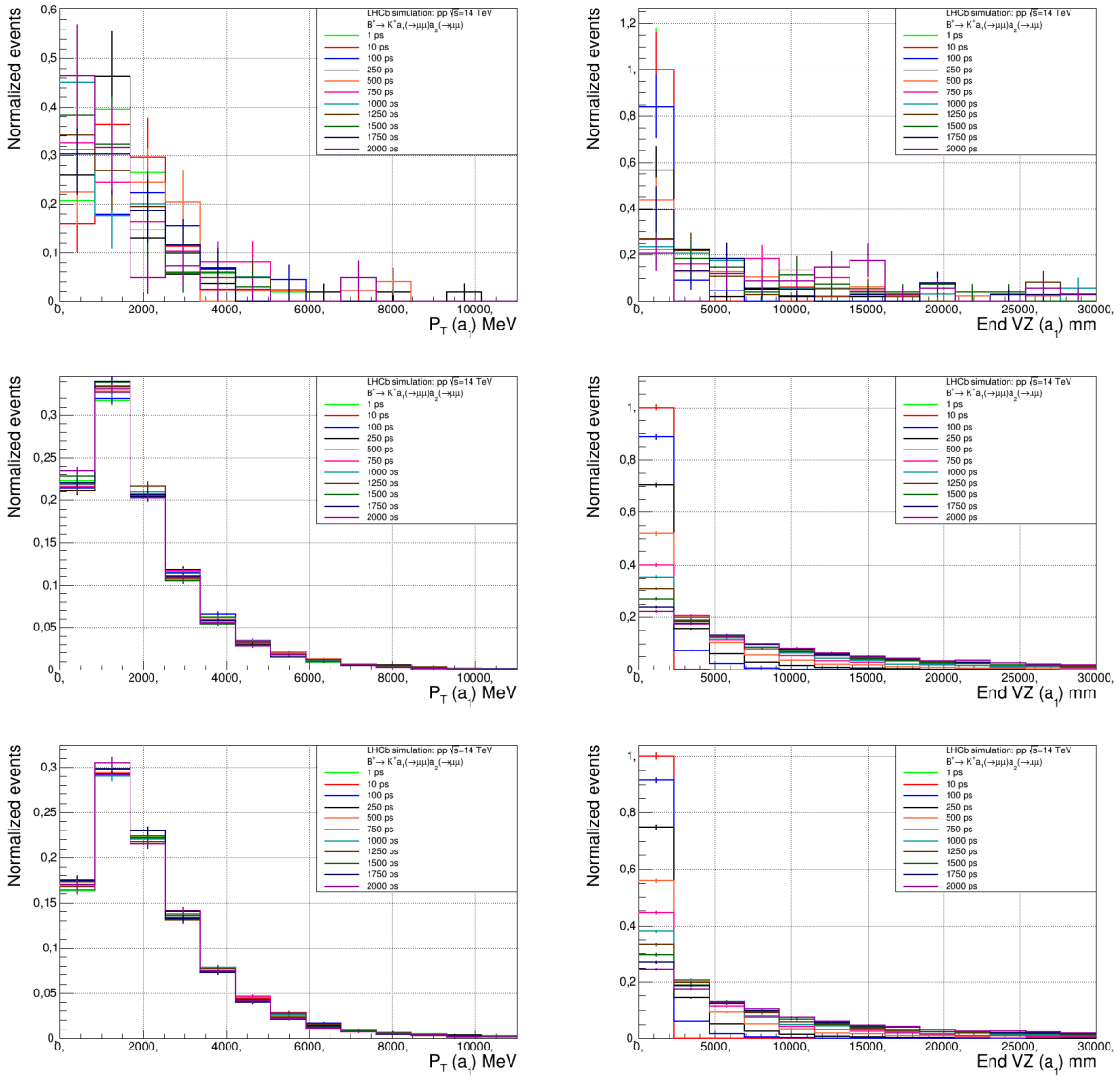

Figure 26: From left to right, from top to botton: transverse momentum distribution and end decay vertex point in the z direction for files with mass of the light scalar from $m = 500$ MeV/c^2 to $m = 1500$ MeV/c^2 as a function of its lifetime.

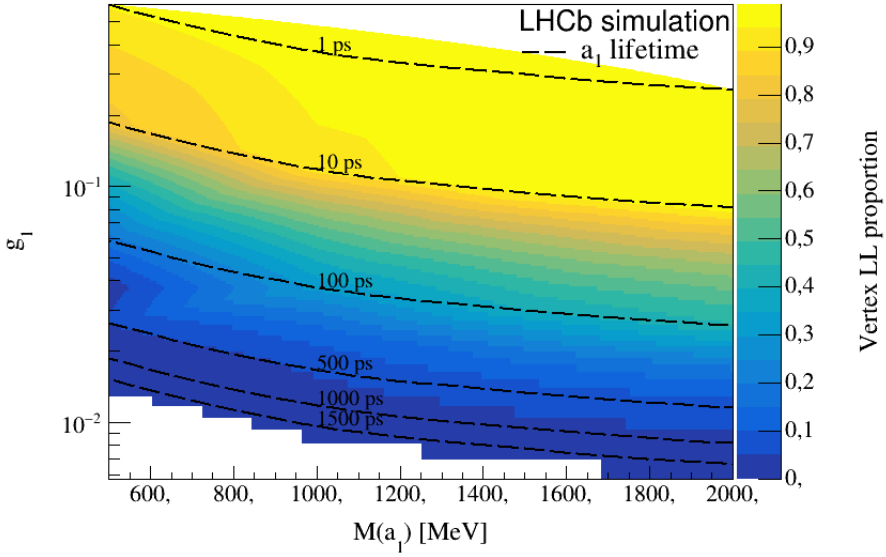

Figure 27: Vertex proportion for LL displaced vertices at reconstructive level for masses vs coupling constant values of the light scalar a_1.

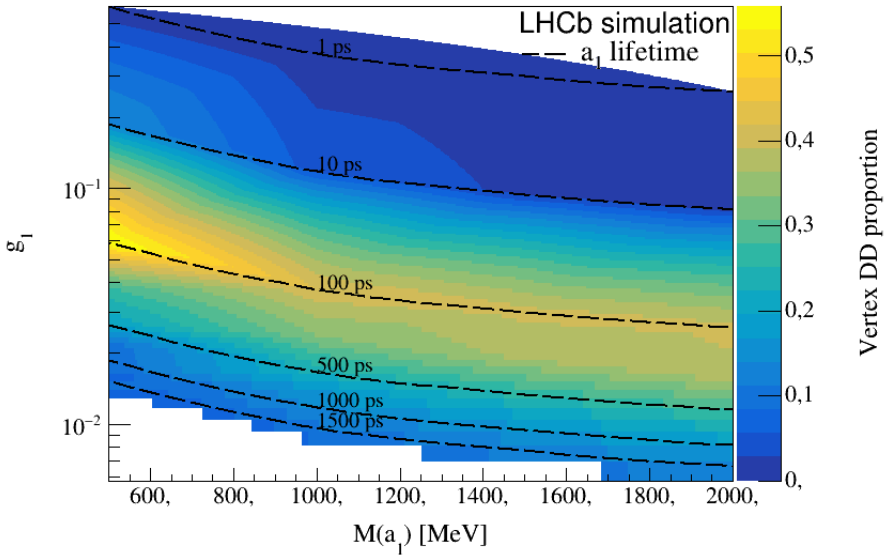

Figure 28: Vertex proportion for DD displaced vertices at reconstructive level for masses vs coupling constant values of the light scalar a_1.

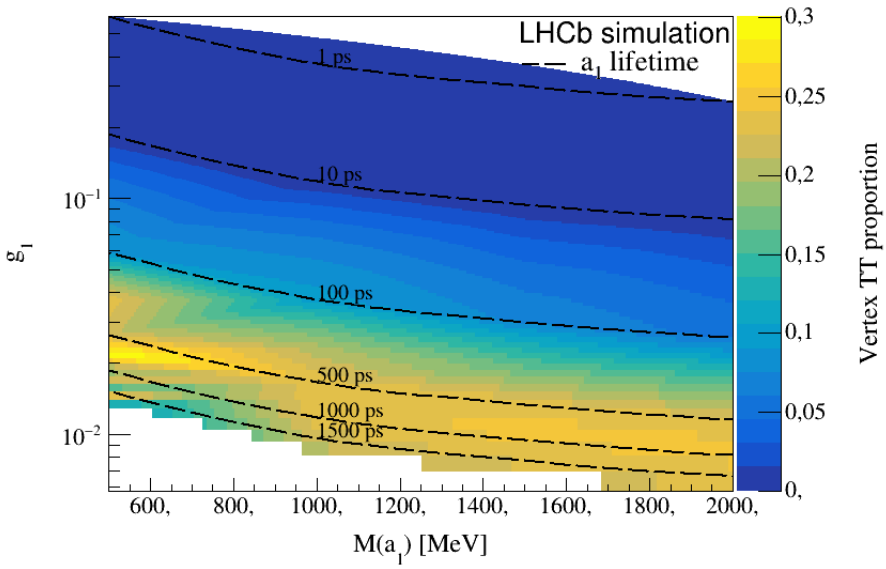

Figure 29: Vertex proportion for TT displaced vertices at reconstructive level for masses vs coupling constant values of the light scalar a_1.

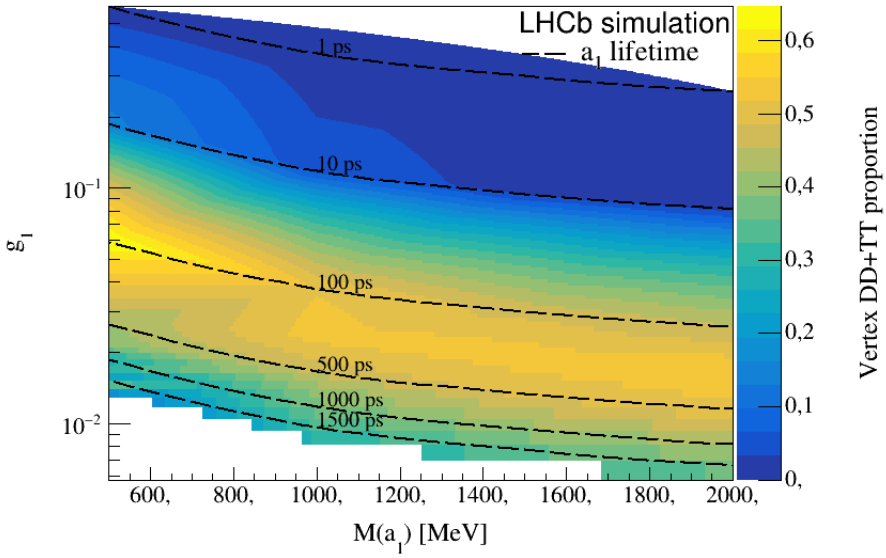

Figure 30: Vertex proportion for DD+TT displaced vertices at reconstructive level for masses vs coupling constant values of the light scalar a_1.

If we compare this model with the Higgs Boson Model, we could see that the region where we miss the information about the Downstream and T-tracks is nearly the same. The main difference is the parameter in the Y axis which in one case is the $sin\theta$ and in the another one is the coupling constant g_1. But all plots seem to show

the same information about that above 10 ps, we are missing relevant information to reconstruct possible events where DD and TT are more present and which can be useful in order to find some signal of LLPs.

6 Conclusions.

A general summary of the actual theoretical and experimental status concerning LLPs signatures has been carried out in this work. We have developed some of the most encouraging frameworks: Composite Higgs, Hidden Valleys, SUSY models with R-parity violation and Dark Photon. The main theoretical concepts and implications were pointed out. Together with this theoretical frameworks, we summarize the main and most updated searches in the LHCb experiment: Dimuon resonances, emerging jets and $e^{\pm}\mu^{\pm}\nu$ decays. On the other hand, two specific analysis were carried out. One taken from the work [4] which give us some context about previous work done in this topic and a second one which is for the first time presented, where a Composite Higgs model is involved. The results obtained highlight the fact that with the current LHCb trigger performance, we are missing relevant information about Downstream and T-tracks. Since the HLT1 trigger stage is only capable of making decisions in terms of Long tracks. The data tell us that an update of such trigger stage to include Downstream and T-tracks in its selection process would highly improve the efficiency of such trigger to detect LLPs.

References

[1] LHCb Collaboration, I. Bediaga, M. C. Torres, J. M. De Miranda, A. Gomes, Massafferri, and et al, "Physics case for an lhcb upgrade ii - opportunities in flavour physics, and beyond, in the hl-lhc era," 2018.

[2] L. Collaboration, "LHCb Tracker Upgrade Technical Design Report," tech. rep., Feb 2014.

[3] LHCb Collaboration, "Trigger Schemes,"

[4] D. Mendoza, "Searching for hidden signatures of physics beyond the Standard Model," Oct 2021.

[5] "LHCb Trigger and Online Upgrade Technical Design Report," tech. rep., May 2014.

[6] D. Curtin, M. Drewes, M. McCullough, P. Meade, R. N. Mohapatra, and et al, "Long-lived particles at the energy frontier: the MATHUSLA physics case," *Reports on Progress in Physics*, vol. 82, p. 116201, oct 2019.

[7] R. Aaij, C. A. Beteta, T. Ackernley, B. Adeva, M. Adinolfi, H. Afsharnia, C. A. Aidala, S. Aiola, and et al, "Searches for low-mass dimuon resonances," *Journal of High Energy Physics*, vol. 2020, oct 2020.

[8] R. Aaij, , C. A. Beteta, T. Ackernley, B. Adeva, M. Adinolfi, and et al, "Search for long-lived particles decaying to $e^{\pm}\mu^{\pm}\nu$," *The European Physical Journal C*, vol. 81, mar 2021.

[9] J. Alexander, M. Battaglieri, B. Echenard, R. Essig, M. Graham, E. Izaguirre, J. Jaros, G. Krnjaic, J. Mardon, D. Morrissey, T. Nelson, Perelstein, and et al, "Dark sectors 2016 workshop: Community report," 2016.

[10] J. Liu, N. Weiner, and W. Xue, "Signals of a light dark force in the galactic center," *Journal of High Energy Physics*, vol. 2015, aug 2015.

[11] D. Craik, P. Ilten, D. Johnson, and M. Williams, "Lhcb future dark-sector sensitivity projections for snowmass 2021," 2022.

[12] D. Curtin, R. Essig, S. Gori, and J. Shelton, "Illuminating dark photons with high-energy colliders," *Journal of High Energy Physics*, vol. 2015, feb 2015.

[13] G. F. Giudice, "Naturally speaking: The naturalness criterion and physics at the LHC," in *Perspectives on LHC Physics*, pp. 155–178, WORLD SCIENTIFIC, jan 2008.

[14] G. Panico and A. Wulzer, *The Composite Nambu-Goldstone Higgs*. Springer International Publishing, 2016.

[15] K. Lane, "Two lectures on technicolor," 2002.

[16] D. B. Kaplan, "Flavor at ssc energies: A new mechanism for dynamically generated fermion masses," *Nuclear Physics B*, vol. 365, no. 2, pp. 259–278, 1991.

[17] L. D. Rold and A. N. Rossia, "The minimal simple composite higgs model," *Journal of High Energy Physics*, vol. 2019, dec 2019.

[18] R. Balkin, M. Ruhdorfer, E. Salvioni, and A. Weiler, "Charged composite scalar dark matter," *Journal of High Energy Physics*, vol. 2017, nov 2017.

[19] A. Blance, M. Chala, M. Ramos, and M. Spannowsky, "Novel b-decay signatures of light scalars at high energy facilities," *Physical Review D*, vol. 100, dec 2019.

[20] M. J. Strassler and K. M. Zurek, "Echoes of a hidden valley at hadron colliders," *Physics Letters B*, vol. 651, pp. 374–379, aug 2007.

[21] A. Pierce, B. Shakya, Y. Tsai, and Y. Zhao, "Searching for confining hidden valleys at LHCb, ATLAS, and CMS," *Physical Review D*, vol. 97, may 2018.

[22] B. Holdom, "Two u(1)'s and ϵ charge shifts," *Physics Letters B*, vol. 166, no. 2, pp. 196–198, 1986.

[23] F. de Campos, O. Éboli, M. Magro, W. Porod, D. Restrepo, M. Hirsch, and J. Valle, "Probing bilinear r-parity violating supergravity at the LHC," *Journal of High Energy Physics*, vol. 2008, pp. 048–048, may 2008.

[24] P. Schwaller, D. Stolarski, and A. Weiler, "Emerging jets," *Journal of High Energy Physics*, vol. 2015, may 2015.

[25] Y. Bai and P. Schwaller, "Scale of dark QCD," *Physical Review D*, vol. 89, mar 2014.

[26] G. Busoni, A. D. Simone, E. Morgante, and A. Riotto, "On the validity of the effective field theory for dark matter searches at the LHC," *Physics Letters B*, vol. 728, pp. 412–421, jan 2014.

[27] S. P. MARTIN, "A SUPERSYMMETRY PRIMER," in *Perspectives on Supersymmetry*, pp. 1–98, WORLD SCIENTIFIC, jul 1998.

[28] L. Lee, C. Ohm, A. Soffer, and T.-T. Yu, "Collider searches for long-lived particles beyond the standard model," *Progress in Particle and Nuclear Physics*, vol. 106, pp. 210–255, may 2019.

[29] C. Csá ki, E. Kuflik, and T. Volansky, "Dynamical r-parity violation," *Physical Review Letters*, vol. 112, apr 2014.

[30] F. Carvalho, O. Éboli, M. Magro, W. Porod, D. Restrepo, S. Das, M. Hirsch, and J. Valle, "Probing neutralino properties in minimal supergravity with bilinear r-parity violation," *Physical Review D*, vol. 86, 06 2012.

[31] R. Aaij, , B. Adeva, M. Adinolfi, Z. Ajaltouni, S. Akar, J. Albrecht, F. Alessio, M. Alexander, and et al, "Updated search for long-lived particles decaying to jet pairs," *The European Physical Journal C*, vol. 77, nov 2017.

[32] A. Kachanovich, U. Nierste, and I. Nišandžić, "Higgs portal to dark matter and $B \to K^*$ decays," *The European Physical Journal C*, vol. 80, jul 2020.